ROLES OF MAVS AND MYD88 IN INNATE AND ADAPTIVE IMMUNE RESPONSES TO RESPIRATORY SYNCYTIAL VIRUS

APPROVED BY SUPERVISORY COMMITTEE

Zhijian J. Chen, PhD

Octavio Ramilo, MD

James Forman, PhD

Nitin Karandikar, MD, PhD

Pinghui Feng, PhD

DEDICATION

To my wife, Elizabeth, and to my parents.

ROLES OF MAVS AND MYD88 IN INNATE AND ADAPTIVE IMMUNE RESPONSES TO RESPIRATORY SYNCYTIAL VIRUS

by

VIJAY GARUD BHOJ

DISSERTATION

Presented to the Faculty of the Graduate School of Biomedical Sciences

The University of Texas Southwestern Medical Center at Dallas

In Partial Fulfillment of the Requirements

For the Degree of

DOCTOR OF PHILOSOPHY

The University of Texas Southwestern Medical Center at Dallas

Dallas, Texas

September, 2008

ACKNOWLEDGEMENTS

I WOULD FIRST LIKE TO THANK MY MENTOR, ZHIJIAN 'JAMES' CHEN, FOR THE SUPPORT THAT HE HAS SHOWN ME DURING MY TRAINING IN HIS LABORATORY. HIS 'DO WHATEVER IT TAKES TO BEST ANSWER THE QUESTION' APPROACH TO RESEARCH FORCED ME TO MASTER A WIDE ARRAY OF LABORATORY TECHNIQUES AND TO BECOME A MORE INDEPENDENT RESEARCHER. MOST IMPORTANTLY, I HOPE THAT THE ENTHUSIASM AND EXCITEMENT THAT HE HAS FOR SCIENCE AND DATA ARE QUALITIES THAT I HAVE PICKED UP FROM HIM. I ALSO THANK THE MEMBERS OF HIS LAB FOR THEIR SUPPORT.

I ACKNOWLEDGE DR. OCTAVIO RAMILO AND MEMBERS OF HIS LABORATORY FOR THEIR GUIDANCE, ASSISTANCE AND FRIENDSHIPS. I AM ALSO INDEBTED TO SO MANY MEMBERS OF THE IMMUNOLOGY PROGRAM AT UTSW WHO HAVE BEEN EXTREMELY GENEROUS TO ME WITH THEIR ADVICE AND REAGENTS.

FINALLY, I THANK MY PARENTS, SISTER (AND FAMILY), AND MY WIFE, ELIZABETH, FOR INVALUABLE EMOTIONAL AND TECHNICAL SUPPORT THROUGHOUT MY TRAINING. I TRULY ENJOYED CONDUCTING EXPERIMENTS ALONG SIDE MY WIFE.

ABSTRACT

Detection of invading viruses by pathogen recognition receptors (PRRs) first illicits an innate immune response which includes the production of anti-viral interferons. TLRs 3, 4, and 7/8 and the RLR, RIG-I, are the primary PRRs involved in the recognition of RNA viruses and they signal through the adaptors TRIF (TLR3, 4), MyD88 (TLR4, 7/8, 9), and MAVS (RIG-I). The innate response serves to limit viral spread and to activate adaptive immune responses which eventually clear the infection. We dissected the contribution of TLR- and RLR- mediated recognition in the host response to Respiratory Syncytial Virus, a common human pathogen. Deletion of *Mavs* abolished the induction of type I interferon (IFN-I) and other pro-inflammatory cytokines by RSV. Genome-wide expression profiling in the lung showed that the vast majority of RSV-induced genes depended on MAVS. Although *Myd88* deficiency did not affect most RSV-induced genes, mice lacking both adaptors harbored higher and more prolonged viral load and exhibited more severe pulmonary disease than those lacking either adaptor alone. Surprisingly, *Myd88*$^{-/-}$*Mavs*$^{-/-}$ mice were able to activate a subset of pulmonary DCs which traffic to the draining lymph node in response to RSV. These mice subsequently mounted a normal cytotoxic T lymphocyte (CTL) response and demonstrated delayed but effective viral clearance. These results

provide an example of a normal and effective adaptive immune response in the absence of innate immunity mediated by MAVS and MyD88.

TABLE OF CONTENTS

PRIOR PUBLICATIONS

Gould MP, Greene JA, Bhoj V, DeVecchio JL, Heinzel FP. Distinct modulatory effects of LPS and CpG on IL-18-dependent IFN-gamma synthesis.
J Immunol. 2004 Feb 1;172(3):1754-62.

Chen ZJ, Bhoj V, Seth RB. Ubiquitin, TAK1 and IKK: is there a connection?
Cell Death Differ. 2006 May;13(5):687-92

Tennakoon DK, Mehta RS, Ortega SB, Bhoj V, Racke MK, Karandikar NJ.
Therapeutic induction of regulatory, cytotoxic CD8+ T cells in multiple sclerosis.
J Immunol. 2006 Jun 1;176(11):7119-29.

Bhoj VG, Chen ZJ. Linking retroelements to autoimmunity. Cell. 2008 Aug 22;
134(4):569-71.

Bhoj VG, Sun Q, Bhoj EJ, Somers C, Chen X, Torres JP, Mejias A, Gomez AM, Jafri H, Ramilo O, Chen ZJ. MAVS and MyD88 are essential for innate immunity but not cytotoxic T lymphocyte response against respiratory syncytial virus. Proc. Natl. Acad. Sci USA. 2008 Sep 16;105(37):14046-51.

Deng L, Dai P, Parikh T, Cao H, Bhoj V, Sun Q, Chen Z, Merghoub T, Houghton A, Shuman S. Vaccinia virus subverts a MAVS-dependent innate immune response in keratinocytes through its dsRNA binding protein E3. J Virology. 2008 Nov; 82(21):10735-46.

Estripeaut D, Torres JP, Somers CS, Tagliabue C, Khokhar S, Bhoj VG, Grube SM, Wozniakowski A, Gomez AM, Ramilo H, Jafri H, Mejias A. Respiratory syncytial virus persistence in the lungs correlates with airway hyperreactivity in the mouse model. J Infect. Dis. 2008 Nov 15;198(10):1435-43.

LIST OF FIGURES

LIST OF DEFINITIONS

SCF-βTrCP – The ubiquitin E3 ligase complex composed of Skp1, Cul1, Roc1 and the F-box protein, βTrCP

ssRNA – Single stranded RNA

dsRNA – Double stranded RNA

CpG – DNA motifs in which a cytosine is followed by, rather than base-paired to, guanine and in which the linking phosphate is un-methylated.

LPS – Lipopolysaccharide, a constituent of the outer wall of gram negative bacteria

MHC – Major histocompatability antigen which are primarily involved in presentation of peptides to T cells

R848 – An imidazoquinoline compound that activates TLR7 and TLR8

CHAPTER ONE

GENERAL INTRODUCTION

The roles of NF-κB and IRF3/7 in viral infection

Within hours of invasion by a viral pathogen, infected cells begin to respond by activating an antiviral gene transcription program. A critical component of the response is induction and secretion of cytokines termed type-I interferons (IFN-I), which includes several IFN-α proteins and one IFN-β (Stark, Kerr et al. 1998) . IFN-I are known to be potent anti-viral cytokines. They are thought to be produced by virtually all nucleated cells in response to viral infection. In addition, all cells are able to respond to IFN-I through the IFN-I receptor, IFNAR, the sole receptor for both IFN-α and IFN- β. IFN-I signal through IFNAR to activate a cascade of JAK-STAT signaling that culminates in the induction of interferon stimulated genes (ISGs) such as chemokines and cytokines that recruit immune cells to the site of infection. Also, cell-intrinsic anti-viral proteins such as MxA, MxB, PKR and OAS are induced; these directly restrict viral replication within the infected cell. PKR is known to phosphorylate eIF2, thus shutting down host translation which is also required for viral protein synthesis and viral replication. OAS synthesizes 2′,5′-oligoadenylates which activate RNaseL, which in turn degrades viral and cellular RNA. Other proteins, for example, inhibit viral

assembly and release from the cell such that this cell autonomous response attempts to block several steps of the virus life cycle to limit its replication.

The critical transcription factors that are activated early after viral infection and that are responsible for the induction of the anti-viral gene program including IFN-I are NF-κB and two members of the interferon regulated factor (IRF) family, IRF3 and IRF7 (Seth, Sun et al. 2006).

NF-κB consists of five members, p65(REL-A), c-REL, REL-B, p50 and p52 (Hayden and Ghosh 2008). All NF-κB transcription factors contain a REL-homology domain (RHD) that is responsible for DNA binding, dimerization, nuclear translocation and IκB binding but only p65, c-REL and REL-B contain a transactivation domain (TAD) which is required for gene activation. p50 and p52 are processed from the precursors p105 and p100, respectively, and must dimerize with a TAD containing member to activate gene transcription. In the inactive state, NF-κB members are regulated by interactions with inhibitory IκB proteins which include the well studied IκBα, IκBβ, IκBε or with IκB-like regions of p105 and p100.

In a healthy uninfected cell, the NF-κB complex p65/p50 is restrained in the cytoplasm through its association with IκB. Upon viral stimulation, signal transduction results in the phosphorylation of IκB on two N-terminal conserved serines. This phosphorylated region is recognized by the SCF-βTrCP ubiquitin E3 ligase complex which, together with an E2, assembles degradative lysine-48 linked ubiquitin chains on the N-terminal of IκB (Chen 2005). Ubiquitinated IκB is then shuttled to the 26S proteasome and degraded. A nuclear localization signal (NLS) is then exposed on NF-κB allowing it to translocate to the nucleus and regulate transcription.

The IRF family constitutes 9 members (IRF-1 through IRF-9) (Tamura, Yanai et al. 2008). At their N-termini, these transcription factors have a DNA binding domain (DBD) that is approximately 150 amino acids long. The DBD binds to DNA regions containing specific motifs known as IFN-stimulated regulatory elements (ISREs) (Stark, Kerr et al. 1998). Each IRF contains an IRF-association domain at the C-terminal which mediates homo- or hetero-dimerization within the IRF family and association with other transcription factors such as signal transducer and activator of transcription (STAT) proteins. Activation of IRFs is achieved by the phosphorylation of C-terminal serine or threonine residues. Phosphorylation is thought to induce a conformational change and subsequent

homo- or hetero-dimerization. Dimers then enter the nucleus to regulate transcription. Key IRFs for the defense against viral infection include IRF3 and IRF7 (Tamura, Yanai et al. 2008).

Activated NF-κB and IRFs may each regulate the expression of genes independently of each other or may cooperate to induce certain genes. The best studied example of their cooperative action is the transcription of the IFN-β gene. The IFN- β gene is under complex regulation that has been relatively well studied. Virus induced transcription of the gene requires that several factors bind to a highly conserved 55 base pair (bp) enhancer region (Maniatis, Falvo et al. 1998). The enhancer contains 4 positive regulatory domains (PRD I-IV). Viral recognition leads to activation of NF-κB, IRF3/IRF7 and through the MAPK pathway, ATF2 and c-Jun. The ATF2/c-Jun complex binds to PRDIV. NF-κB, made up of p65 and p50, binds to PRDII and the IRFs bind to ISREs in the central PRDI-III region. This complex has been termed the IFN-β enhanceosome. Along with the structural protein HMG I(Y) and the transcriptional co-activator CBP/p300, and other basal transcription machinery, the enhanceosome drives IFN-β transcription (Thanos and Maniatis 1995).

As mentioned, IFN-β secreted from the virally infected cells engages the IFNAR on the secreting cell as well as its neighbors to then induce JAK-STAT signal transduction. This leads to phosphorylation and activation of STAT1, STAT2 and IRF9 which, together, form the ISGF3 complex. In turn, ISGF3 activates the transcription of ISGs including the IFN-α family through binding to ISRE elements in their promoters. Signaling through the JAK-STAT pathway constitutes the secondary response amplifying the antiviral gene program. The primary response is the initial induction of genes by NF-κB and IRF3. NF-κB can, for instance, activate pro-inflammatory cytokines such as IL-6, IL-1 and TNF-α.

Viral detection by PRRs

Activation of NF-κB and IRFs occurs in response to pathogen detection by our innate immune system. Direct detection is mediated by germline-encoded receptors which bind to pathogen associated molecular patterns (PAMP), elements of pathogens which are essential for their survival and typically distinct from our own molecules. PAMPs come in many forms including lipids, lipoproteins, proteins, and nucleic acid elements and are usually shared among classes of microbes (e.g. RNA viruses, gram negative bacteria). Upon PAMP binding to host receptors, collectively termed pathogen recognition receptors

(PRR), signaling pathways are activated, leading to the induction of various anti-pathogen measures.

The most well studied family of PRRs is the Toll-Like Receptors (TLR). This family consists of 12 members in humans (TLRs 1-9, TLR 11-13) (Kawai and Akira 2006). TLRs are characterized by a ligand binding Leucine Rich Repeat region (LRR) followed by a single pass transmembrane domain and then by a cytoplasmic tail containing a signaling Toll-IL-1 Receptor (TIR) domain, which mediates interactions with signaling adaptors. TLRs are often subdivided based on their cellular localization; endosomal TLRs (TLRs 3, 7/8, 9) traffic from the ER to endosomal compartments where they engage luminal PAMPs from endocytosed microbes. The remaining TLRs are situated on the plasma membrane with the LRR facing the extracellular space. Each TLR recognizes a distinct PAMP (e.g. lipoprotein: TLR2+TLR1/6; LPS: TLR4; dsRNA: TLR3; CpG DNA: TLR9; flagellin: TLR5) and together they cover a broad array of pathogens including bacteria, viruses, fungi and protists. Signaling initiated by these receptors culminates in the activation of NF-κB and in certain cases (TLRs 3, 4, 7/8, and 9) IRF3, which induce the innate anti-microbial gene program.

Another group of PRRs are the Nod-like Receptors (NLRs) (Kanneganti, Lamkanfi et al. 2007). The NLRs are a large family of cytosolic proteins that

largely conform to a tripartite structure. A central nucleotide-binding domain (NBD; also known as NACHT domain) is believed to bind ATP and mediate oligomerization. A C-terminal LRR region is thought to sense PAMPs or participate in autoinhibition, depending on the NLR. At their N-termini, NLRs also possess a CARD, PYD, BIR, or Acidic activation Domain (AD). This region is involved in the recruitment of downstream signaling proteins. Two of the most studied NLRs, NOD1 and NOD2, are enriched in the gut where they detect the presence of peptidoglycans (PG) derived from the bacterial cell wall. NOD1 and NOD2 activation also leads to NF-κB induction. Other NLR members have also been implicated in pathogen recognition. Members of this group, which include NLRP1 (Nalp1b), NLRP3 (Nalp3) and NLRC4 (IPAF), form complexes with the adaptor ASC, termed the inflammasome. Inflammasomes lead to processing and secretion of the cytokines IL-1β and IL-18. NLRC4 has been shown to detect flagellin from Legionella and Salmonella independent of TLR5, while NLRP1 detects anthrax lethal toxin. NLRP3 has been shown to initiate signaling in response to a variety of PAMPs including LPS, MDP, dsRNA, and even certain types of DNA although there is no evidence that it serves directly as the receptor for these microbial components.

A third group of PRRs also resides in the cytoplasm. The three members RIG-I, MDA5 and LGP2, collectively called RIG-I-like receptors (RLRs), are thought to

be expressed in most cells types where they participate in viral sensing (Lee and Kim 2007). These receptors directly bind viral dsRNA or uncapped-5' triphophorylated regions of viral mRNA (Hornung, Ellegast et al. 2006; Pichlmair, Schulz et al. 2006; Bowie and Fitzgerald 2007). A central RNA helicase domain and a C-terminal regulatory domain (RD) cooperate in the binding of these ligands (Saito, Hirai et al. 2007). In addition to these domains, RIG-I and MDA5 also contain tandem CARD domains at their N-termini which are presumed to participate in interactions with an essential downstream signaling CARD containing adaptor, MAVS (also known as IPS-1, VISA and CARDIF) (Meylan, Curran et al. 2005; Seth, Sun et al. 2005; Taro Kawai 2005; Xu, Wang et al. 2005). LGP2, however, lacks N-terminal CARDs and has been proposed to exert a regulatory effect on RIG-I and MDA5 signaling either as an RNA sink or through direct binding to the other two receptors (Rothenfusser, Goutagny et al. 2005; Horvath 2006). Much like TLRs, signaling from RIG-I and MDA5 activates NF-κB and IRF3 leading to anti-microbial gene induction.

With respect to sensing RNA viruses, TLRs 3 and 7, and the RLRs are considered most important as they bind viral dsRNA and ssRNA (Fig. 1). Binding viral RNA within endosomes by the TLRs ensures that they are not activated by host cytosolic RNA such as mRNA. In the case of cytosolic RLRs, an affinity for uniquely viral RNA features (dsRNA and uncapped 5' triphosphate regions)

ensures pathogen specificity as host mRNA are single-stranded and contain a 5' cap structure.

PRRs may be expressed both on non-immune as well as immune cells. Epithelial cells, often the first cells to be infected, are known to contain distinct subsets of PRRs (RLRs, NOD1 and 2, and a limited array of TLRs). In response to pathogen detection, these cells secrete chemokines to recruit immune cells and can also initiate cell intrinsic defenses to limit pathogen replication.

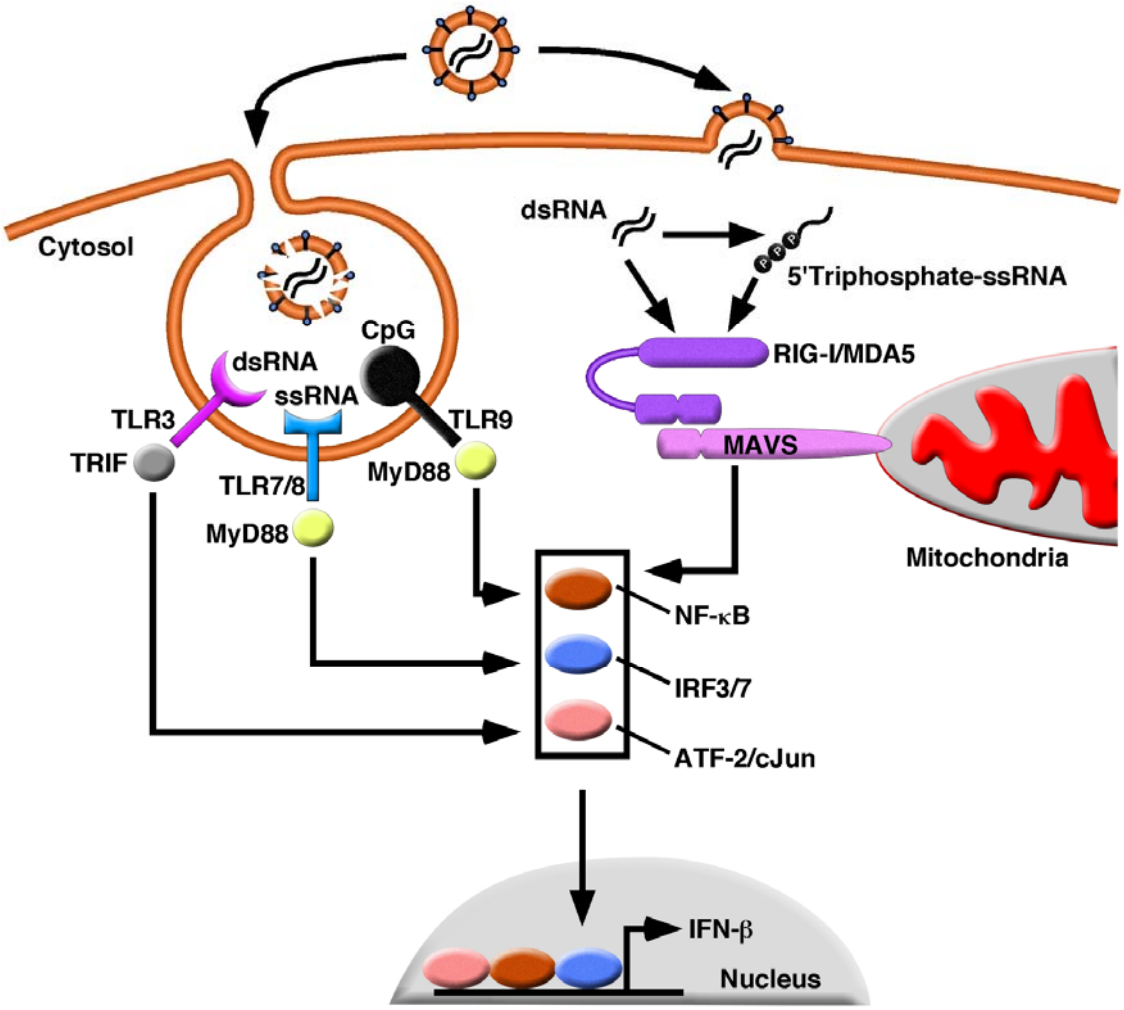

Figure 1. Mammalian immune systems employ TLRs and RLRs in order to detect nucleic acids. TLRs 3, 7/8, and 9 bind to viral dsRNA, ssRNA, and CpG DNA within endosomes. Upon engagement, these receptors signal through TRIF (TLR3) or MyD88 (TLR7/8 and TLR9) to activate the transcription factors NF-κB, IRF3/7, and ATF-2/c-Jun. These activated factors enter the nucleus and induce the transcription of antiviral genes including IFN-β. Alternatively, viral dsRNA and uncapped 5'-triphosphate RNA in the cytosol are detected by the RNA helicases (RLRs) RIG-I and MDA-5, respectively. Once bound to their ligands, these receptors transmit an activation signal to their common adaptor, MAVS, located on the mitochondrial surface. MAVS relays the signal to ultimately activate NF-κB, IRF3/7, and ATF-2/c-Jun, also resulting in antiviral gene induction.

Immune cells such as macrophages and dendritic cells (DCs) express a wide variety of PRRs (NODs, RLRs, and a wide array of TLRs) . Activation of TLRs on macrophages, for example, promotes their ability to engulf and degrade microbes (Iwasaki and Medzhitov 2004). Both macrophages and myeloid DCs [mDCs; also known as conventional DC (cDC)] are robust producer of inflammatory cytokines and chemokines such as TNF-α, IL-6, and MCP-1 when activated by PAMPs. PRR activation in mDCs in particular also promotes their ability to degrade microbes and present degraded microbial proteins on their surface in the form of T cell epitopes bound to MHC. This important function is crucial for the initiation of adaptive T cell responses to pathogens. Notably, in DC, up-regulation of many proteins involved in antigen processing, presentation and T-cell activation is downstream of PRR and NF-κB activation.

Plasmacytoid dendritic cells (pDCs), another subset of DCs, are thought to be major producers of IFN-I and are thus key anti-viral cells (Liu 2005). In contrast to other cells, they constitutively express high levels of IRF7 which, in part, confers on them the ability to rapidly induce IFN-I (Izaguirre, Barnes et al. 2003). pDC are thought not to utilize RLRs and depend on endosomal TLRs to detect viruses (Kato, Sato et al. 2005).

Specific TLR and RLR signaling cascades

As this work centers on specific TLR (TLR 3, 4, 7) and RLR (RIG-I) activation, a more detailed account of signaling in the pertinent pathways follows.

TLR 3, 4, 7/8 signaling

TLRs contain a cytoplasmic signaling Toll-IL-1R domain so named because a similar domain is found in the IL-1R cytoplasmic region (Kawai and Akira 2006). TLRs transduce signals from their TIR through two essential cytosolic TIR containing adaptor proteins, MyD88 and TRIF. With the exception of TLR3, all TLRs employ MyD88 to transduce signals. TLR3 signals through TRIF. TLR4 is the exceptional receptor signaling separately through both MyD88 and TRIF, while all others use only one or the other.

Signals from TLRs 3, 4 and 7 culminate in the activation of two groups of kinases (Seth, Sun et al. 2006). One is the IκB kinase (IKK) complex, which comprises two catalytic subunits, IKK-α and IKK-β, and a regulatory subunit, NEMO (also known as IKK-γ/IKKAP). Upon activation, the IKK complex phosphorylates IκB. Phosphorylated IκB is then ubiquitinated and degraded by the proteasome. This relieves inhibition on NF-κB so that it enters the nucleus. The other group that is activated consists of the IKK-related kinases TBK-1 and IKKε (Fitzgerald,

McWhirter et al. 2003). These are thought to function redundantly to phosphorylate and activate IRF3.

Once TLR4 binds to LPS in association with CD14, its TIR interacts with the TIR domains of MyD88 and TRIF (Kawai and Akira 2006). MyD88 additionally contains a Death Domain (DD) which permits homotypic interactions to recruit the DD containing proteins of the IRAK family. IRAK4 recruited to the receptor complex phosphorylates threonine residues on IRAK1. This activates IRAK1 and leads to its autophosphorylation and resultant dissociation from the MyD88 signaling complex. IRAK1 then interacts with and activates the E3 ligase, TRAF6. TRAF6 catalyses the formation of lysine-63 linked (K63) ubiquitin chains to itself and downstream proteins (Chen 2005). These ubiquitin chains recruit the TAK1 kinase complex (TAK-1, TAB1, TAB2/3) via the ubiquitin binding proteins TAB2/3. The kinase activity of recruited TAK1 is then activated. TAK1 then phosphorylates IKK-β, thus activating the IKK complex. Ultimately this leads to NF-κB activation. TAK1 is a MAPKKK and also activates the MAPK pathway, leading to p38 and JNK activation.

TRIF, on the other hand, interacts with another TRAF family member, TRAF3, which, through a yet unknown mechanism, activates TBK-1/IKKε. This, in turn, leads to IRF3 phosphorylation and activation. TRIF can also interact with TRAF6

leading to NF-κB activation. This path to NF-κB constitutes a late phase of activation of the transcription factor, whereas the MyD88 path is the early phase.

TLR3 and TLR7 reside in endosomes with their ligand-binding regions facing the luminal side and their signaling portions facing the cytosol. When viruses, such as influenza virus, enter a cell through the endosomal route, viral RNA exposed during vesicle acidification is detected by the cognate TLR. Once bound to their ligands, TLR3 and TLR7 activate TRIF and MyD88, respectively. In the case of TLR3, TRIF leads to both IKK-NF-κB activation and TBK-1/IKKε-IRF3 activation similarly to the TRIF pathway downstream of TLR4 (Yamamoto, Sato et al. 2003). TLR7, which is primarily expressed in pDCs, engages MyD88 which leads to TAK1 activation through TRAF6. This leads to NF-κB and MAPK activation. Interestingly, it has been shown that, in pDCs, MyD88 can also form a complex with IRAKs 1 and 4, TRAF6, TRAF3 and, importantly, IRF7. In this complex, IRAK1 directly phosphorylates IRF7 to activate it. This results in robust IFN-α induction in these cells.

RIG-I signaling

In the cytosol, RIG-I bind dsRNA and uncapped 5'-triphosphate regions of RNA formed during viral replication and transcription (Fig. 2). Unstimulated RIG-I is

held in an auto-inhibited state due to an interaction between a C-terminal repressor domain (RD) and the N-terminal CARDs (Saito, Hirai et al. 2007). Upon binding the ligands through the RNA helicase and repressor domains, the molecule is thought to undergo a conformational change which releases the CARDs from the RD. The CARDs are thought to relay an activation signal to the CARD-containing adaptor, MAVS through homotypic CARD-CARD interactions. MAVS has been shown to interact with TRAF2, 3, and 6 (Xu, Wang et al. 2005; Saha, Pietras et al. 2006). TRAF3 is thought to lead to TBK-1/IKKε activation and $TRAF3^{-/-}$ cells lose the ability to activate IRF3 after stimulation of the RLR pathway. TRAF2 or 6 are thought to convey signaling to the IKK complex although the mechanism is unclear (Xu, Wang et al. 2005).

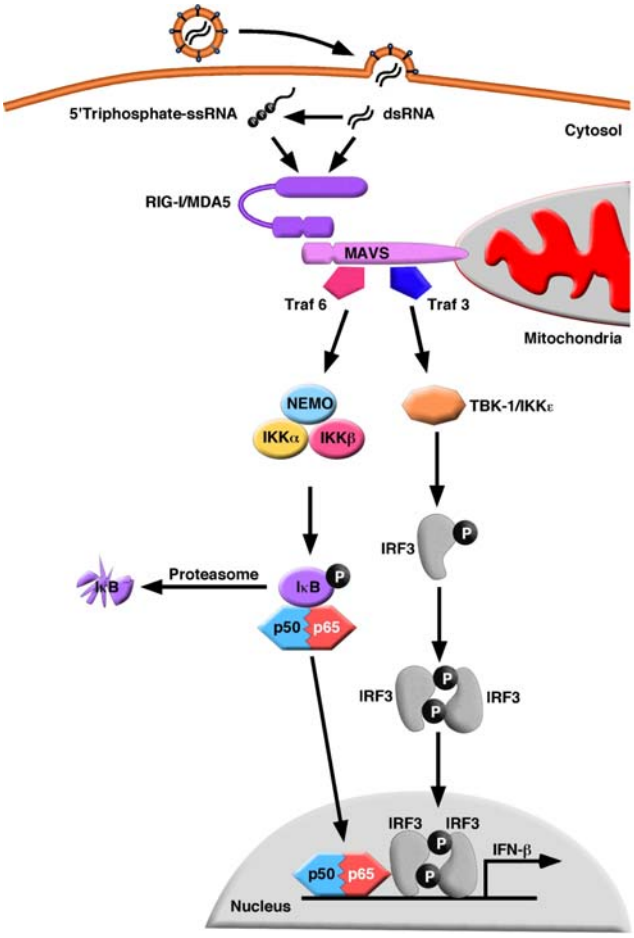

Figure 2. MAVS transmits activation signals from RLRs to activate NF-κB and IRF3, resulting in transcription of IFN-β. RIG-I and MDA-5 bind viral RNA containing 5'-triphosphate and dsRNA, respectively, in the cytosol. The ligand-bound receptors then interact with MAVS through CARD-CARD interactions. MAVS subsequently binds to the adaptors TRAF6 and TRAF3. TRAF6 then activates the IKK complex, leading to the phosphorylation of IκB. IκB is then ubiquitinated and degraded by the proteasome, releasing NF-κB from inhibition. NF-κB translocates to the nucleus to induce genes including IFN-β. TRAF3 induces the activation of the IKK-related kinases TBK1 and IKK-ε, which, in turn, phosphorylate IRF3. Phosphorylated IRF3 forms a homodimer, which enters the nucleus to form an enhanceosome complex together with NF-κB to induce IFN-β transcription.

Dendritic cells at immune interfaces

DCs are unique immune cells that play critical roles in both the innate and adaptive phases of immunity. In fact, DCs activated during the innate phase are directly responsible for activation of adaptive $CD4^+$ and $CD8^+$ T cells and they are thus considered to bridge the two immune phases (Banchereau and Steinman 1998). DCs actually constitute a family of various subsets. However, for simplicity sake, they will be divided into two subsets in this thesis: myeloid DCs (mDCs) and plasmacytoid DCs (pDCs). Whereas pDC are considered to primarily secrete cytokines, mDC are thought to be more important for T cell activation as will be discussed below.

mDCs can be found at interfaces between the body and the outside environment such as in the skin, lungs, or GI tract. At these sites, they actively take up extracellular material by phagocytosis and pinocytosis in order to survey their environment. In the event that pathogens or PAMPs are taken up, or when they are actively infected, their PRRs become activated. As discussed, this can lead to rapid cytokine and chemokine production and secretion which promotes further innate immune responses. Additionally, activated DCs begin to leave their peripheral tissue site, enter nearby lymphatic vessels and journey to draining lymph nodes.

During their migration, DCs process the protein component of their pathogen cargo into peptides that can be presented as antigen on MHC-I and MHC-II to activate T cells. They upregulate several components of the protein machinery involved in processing and presentation of antigen including the MHC molecules themselves. Once at lymph nodes, they are primed to interact with and activate antigen specific T cells via MHC-TCR interactions.

Activation of antigen specific T and B cells

Mature, naïve T cells are first activated by DCs in the lymph node in a process called priming. Most important for both $CD4^+$ and $CD8^+$ T cell activation is MHC-peptide ligation of the TCR (signal 1) and the engagement of co-stimulatory ligands on the DC by T cell costimulatory receptor (signal 2). Signaling through co-stimulatory receptors synergizes with TCR signaling, resulting in most optimal activation. In the context of TCR engagement, lack of engagement of costimulatory ligands such as CD80 and CD86 (B7.1, B7.2) by their receptor CD28 on naive T cells results in insufficient activation of the T cell (Schwartz 2003). The T cell may undergo cell death or enter an unresponsive, anergic state rather than develop effector functions. The signals required to activate $CD4^+$ T cell are better understood than the requirements for proper $CD8^+$

T cell priming. In addition to APCs, $CD8^+$ T cells may require the direct or indirect help of activated $CD4^+$ T cells (Prlic, Williams et al. 2007). Alternatively, inflammatory cytokines such as IL-12 or IFN-I acting on the $CD8^+$ T cells (signal 3) may substitute for $CD4^+$ T cell help (Williams and Bevan 2007).

B cell activation occurs upon direct antigen recognition by the B cell receptor (BCR). Antigen binding results in antigen uptake, processing and MHC-II mediated presentation of antigen-derived peptides on the surface of the B cell. In the lymph node, DC-activated $CD4^+$ T cells interact with antigen presenting B cells through TCR-peptide-MHCII interactions (Parker 1993). During this interaction, $CD4^+$ T cells provide further stimulation to B cells through CD40-CD40L binding. These fully activated B cells go on to mature into antibody-producing plasma cells.

CHAPTER TWO

THE ROLES OF MYD88 AND MAVS IN RSV DISEASE AND INNATE IMMUNITY

Introduction

RSV disease

Infection with Respiratory Syncytial Virus (RSV) is recognized as one of the most important pathogens causing respiratory illness in infants worldwide. By 2 years of age, nearly all individuals have been infected with RSV (Parker 1993). In most, RSV disease usually occurs as a mild upper respiratory illness which includes fever, cough, rhinorrhea, and nasal congestion. However, in 25-40% of infants or young children, RSV causes a lower respiratory tract infection (LRTI), leading to pneumonia and bronchiolitis that are a significant cause of morbidity and mortality (Welliver 2003). It is estimated that between 2-3% of patients with LRTI are hospitalized. Infants with congenital heart defects, chronic lung disease of prematurity, and immune deficiency are at an increased risk of developing severe RSV disease requiring hospitalization. Prematurely born infants are also at a higher risk of experiencing more severe disease due in part to incomplete lung development and to lower levels of maternal antibodies. Early RSV infection is also associated with the development of asthma later in life (Openshaw, Dean et al. 2003).

It is now known that RSV infection is not limited to infants and young children, but can occur repeatedly throughout life due to incomplete immunity generated against the virus even in generally healthy individuals. Fortunately, RSV infection in adulthood usually manifests as a mild upper respiratory tract illness. However, in certain high-risk groups such as the immune-compromised and the elderly, RSV infection is a significant problem. RSV is second to influenza as a viral pathogen causing serious illness in adults over 65 years and it is estimated that, in the U.S., around 10,000 deaths in this group can be attributed to RSV infection (Murata and Falsey 2007).

Treatment of established RSV disease primarily consists of supportive care including oxygen and fluids rather than antiviral treatments. Polyclonal human anti-RSV IgG(RSV-IGIV) and a humanized monoclonal anti-RSV antibody (Palivizumab) are currently used as prophylaxis for high-risk children. There is no RSV vaccine in current clinical use. A vaccine trial in the early 60's using formalin-inactivated RSV resulted in more severe disease in vaccinated children compared to controls upon subsequent encounter with the live virus (Kim, Canchola et al. 1969). Numerous studies since then have shown that failure of the vaccine was likely due to lack of induction of neutralizing antibodies and to over-exuberant Th2 induction. Modeling of the vaccine-promoted-disease in mice

implicated Th2 cells and eosinophil activation and excess IL-4 and IL-5 production in exacerbated symptoms (Connors, Kulkarni et al. 1992; Connors, Giese et al. 1994; Waris, Tsou et al. 1996). Development of a vaccine is clearly complicated by the fact that the host response to the virus contributes to the disease. The previous failure underscores the importance of a better understanding of the host response to the virus for the design of safe and effective treatment and prophylaxis (Collins and Murphy 2005).

RSV virology

RSV belongs to the Paramyxovirus family of negative-sense ssRNA viruses along with the widely used virus, Sendai Virus (SeV) (Hall and McCarthy 2004). RSV is further classified in the Pneumovirus genus and consists of two subtypes, A and B which differ mainly in their G, F, SH and NS1 proteins. The virus consists of an approximately 15-kilobase non-segmented RNA genome which is bound by the polymerase complex and nucleoprotein, and the nucleocapsid. Ten monocistronic, capped, and polyadenylated mRNAs are transcribed in the host cell cytoplasm. Each mRNA encodes a viral protein except for the M2 transcript which contains two overlapping ORFs, M2-1 and M2-2. The nucleocapsid is surrounded by a viral envelope – a lipid bilayer derived from a host cell.

The RSV envelope contains the fusion protein (F), attachment protein (G), and a small hydrophobic protein (SH) (Hall and McCarthy 2004). The G glycoprotein promotes initial attachment to host cells and the F protein subsequently induces the fusion of the envelope with the host's plasma membrane. G protein is not absolutely required for attachment, however, and may serve to increase the efficiency of the process. The cellular receptor for G protein is not currently known. Cell surface GAGs and the chemokine receptor CX3CR1 have been proposed as candidates. Upon membrane fusion, the viral nucleocapsid is delivered directly into the cytoplasm. The F protein is also responsible for fusion of the infected host cell membrane with the membrane of neighboring cells, which results in syncytia and viral spread. Viral progeny leave the cell either by fusion with an adjacent cell or upon rupture of the host cell.

It is within the host cytoplasm that both transcription and replication of the viral genome occur (Hall and McCarthy 2004). The idea that secondary structures within viral RNA or replicative intermediates may serve has PAMPs is certainly applicable to RSV. Transcription of RSV ORFs results in mRNAs containing a modified 5' cap (Cowton, McGivern et al. 2006).

TLRs and RLRs in the response to RSV

As introduced earlier, the most important viral PRRs include the RLRs and a family of TLRs, namely TLR3, TLR7, TLR9, and TLR4. With respect to RSV, TLR9 likely does not contribute as it is specific for unmethylated CpG motifs in DNA which are not produced at any stage of the RSV life cycle.

TLR4, the first TLR implicated in RSV recognition, was found to bind the F protein (Kurt-Jones, Popova et al. 2000). Recognition of F through TLR4 was shown to induce IL-6 production in macrophages in a manner dependent on CD14. It was also shown that C57BL/10ScCr (ScCr) mice harboring a deletion in *Tlr4* were defective in RSV clearance as early as 5 days after infection. Studies in C57BL/10ScNCr (ScNCr)mice, progenitors of C57BL/10ScCr carrying the same *Tlr4* mutation, found delayed viral clearance and decreased NK cell recruitment and function compared to control mice only late (day 11) after RSV infection (Haynes, Moore et al. 2001). These experiments were complicated by the fact that ScCr mice also contain a mutation in IL-12Rb2, rendering them hypo-responsive to IL-12 which stimulates IFN-γ production. A subsequent systematic study using mice with single *Tlr4* or *Il-12rb2* mutations or both mutations found no role for TLR4 in the anti-RSV response (Ehl, Bischoff et al. 2004). In the same study, NK-cell recruitment and viral clearance were slightly impaired in *Il-12rb2* single mutant mice compared to WT controls. A study comparing C3H/HeN (WT) and C3H/HeJ (*Tlr4*-deficient) mice also found no role for the receptor in the response

to a related pneumovirus, pneumonia virus of mice (PVM) (Faisca, Tran Anh et al. 2006). Recently, however, studies have found associations between the severe RSV disease in humans and mutations within the *Tlr4* locus (Awomoyi, Rallabhandi et al. 2007; Tulic, Hurrelbrink et al. 2007). Taken together, it is unclear what, if any, role TLR4 plays in the immune response to RSV.

The RSV genome is a ssRNA molecule which can potentially serve as a ligand for TLR7. However, the role of TLR7 in the detection of RSV has not yet been studied. The finding that antecedent RSV infection can inhibit IFN-α production by human pDCs stimulated with R848 suggested that TLR7 may play a role in detecting RSV as its downstream signaling seems to be actively targeted by the virus (Schlender, Hornung et al. 2005). However, the RSV-mediated inhibition is not be specific as the same strain also inhibits TLR9 mediated IFN-α induction in pDC. In short, the importance of TLR7 in the anti-RSV response is not known.

Studies have determined that TLR3 transcription is induced by RSV infection both in vitro using respiratory epithelial cells as well as in mouse lungs. In vitro, TLR3 knockdown by siRNA indicated no role in the control of viral replication (Rudd, Burstein et al. 2005). However, TLR3 seemed to mediate secretion of certain chemokines such as CCL5, CXCL8 and CXCL10 as well as IFN-β. In vivo, too, deletion of *Tlr3* had no impact on control of viral replication (Rudd,

Smit et al. 2006). However, mice lacking this receptor demonstrated a Th2-shifted immune response to RSV compared to WT mice. The response was characterized by more mucus production, pulmonary eosinophilia, IL-5 and IL-13. Interestingly, *Myd88*$^{-/-}$ mice demonstrated a similar response with no effect on viral load, greater mucus production and IL-4, IL-5 and IL-13 (Rudd, Schaller et al. 2007). *Myd88*$^{-/-}$ mice also produced lower amount of IFN-γ compared to WT counterparts, in contrast to *Tlr3*$^{-/-}$ mice which were normal in regard to this cytokine. The receptor transducing MyD88 mediated signals was not explored and must be distinct from TLR3.

RLR recognition of RSV has only been studied in vitro in a limited set of cell types. Using *Rig-i*$^{-/-}$ mouse embryonic fibroblasts (MEFs), RIG-I was confirmed to be a receptor for RSV mediating IFN-I and IFN-stimulated gene (ISG) induction (Loo, Fornek et al. 2007). Cells lacking *Mda-5* were normally responsive to RSV. In response to other RNA viruses such as SeV, Vesicular Stomatitis virus (VSV), and Newcastle Disease virus (NDV), RLRs are dispensable for normal IFN-I responses in pDC but crucial in all other cell types tested (Kato, Sato et al. 2005; Kumagai, Takeuchi et al. 2007). As expected, the in vivo dependence on MAVS signaling for innate responses is more complex. As will be discussed later, compensatory MyD88 dependent innate responses have

been observed after virus infection of MAVS-deficient mice (Kumagai, Takeuchi et al. 2007).

Hypotheses and Aims

At the time this study was begun, there was no data on the role of RLRs in the response to RSV in vitro or in vivo. We hypothesized that MAVS, an essential adaptor for RLRs, mediates signaling after receptor-recognition of RSV and is essential for an innate cytokine response to the virus. As a corollary, we hypothesized that loss of MAVS-mediated responses would significantly impair viral clearance and thus increase disease severity.

Our aims to test this hypothesis were to

1. Infect several cell types (pDC, cDC, macrophages, MEFs, lung fibroblasts) from WT and *Mavs*$^{-/-}$ mice in vitro with RSV and test their response by measuring secreted IFN-I.
2. To infect WT, *Mavs*$^{-/-}$, *Myd88*$^{-/-}$, and *Mavs*$^{-/-}$*Myd88*$^{-/-}$ (double knockout, DKO) mice intranasally with RSV and measure cytokines secreted locally and systemically and early mRNA induction in the lung.

3. Measure viral titers, airway obstruction, and lung histopathology at various times after infection as markers of viral control and disease in WT, *Mavs*$^{-/-}$, *Myd88*$^{-/-}$, and DKO mice infected with RSV.

Material and Methods

Mice

The generation of *Mavs*$^{-/-}$ mice has been described previously (Sun, Sun et al. 2006)(Sun, Sun et al. 2006). Briefly, *Mavs*$^{-/-}$ mice were made by homologous recombination with a targeting vector in 129/Sv ES cells, which were then injected into C57Bl/6 blastocysts to create chimeric mice. *Myd88*$^{+/-}$ mice, which had been backcrossed to the C57Bl/6 background, were kindly provided by Dr. Shizuo Akira (Osaka University). To obtain mice lacking *Mavs*, *Myd88*, or both (DKO), *Mavs*$^{+/-}$ and *Myd88*$^{+/-}$ mice were bred with each other and the resulting progeny with appropriate genotypes were used in the experiments. All of the mice described in this report were engineered and housed in animal facilities at the University of Texas Southwestern Medical Center and the experimental protocols were approved by the Institutional Animal Care and Use Committee.

Viruses

Sendai virus (SeV; Cantell strain) and vesicular stomatitis virus (VSV) have been described previously (Seth, Sun et al. 2005; Sun, Sun et al. 2006)(Seth, Sun et al. 2005; Sun, Sun et al. 2006). RSV (strain A2) was propagated and quantified by plaque assay using HEp-2 cells as previously described (Jafri, Chavez-Bueno et al. 2004).

In vivo infection

Mice were anesthetized with inhaled isofluorane before intranasal inoculation with 10^7 PFU of live RSV in 100 μL of EMEM supplemented with L-glutamine, HEPES, penicillin, streptomycin, and 10% FBS. Control animals were sham-inoculated with 100 μL of cell-culture media.

Cytokine measurements

IFN-α and IFN-β were measured using mouse IFN-α and mouse IFN-β ELISA kits (Pestka Biomedical Laboratories). IL-1β was also measured by ELISA (Pierce). IL-6, TNF-α, MCP-1, IL-12, IL-10 and IFN-γ were measured using the BD Mouse Inflammation Cytometric Bead Array (CBA) Kit and a FACSCalibur. IFN-γ was also measured using ELISA MAX (BioLegend) where indicated.

Cells

Lung fibroblasts were prepared according to published procedures (Yamamoto, Sato et al. 2003). Bone marrow cells were prepared by flushing femurs and tibiae of mice. Cells were cultured in RPMI 1640 containing 10% FBS, 10mM HEPES (pH 7.4), 50 μM β-mercaptoethanol, and 100 ng/ml human Flt3 ligand (peproTech) or 10 ng/ml murine GM-CSF (peproTech). Fresh media with a growth factor was added to cultures on day 3 or 4. After 6–8 days, the cells were collected and used as Flt3L-induced BMDCs or GM-CSF-induced BMDCs, respectively. Flt3L-induced BMDCs were used as bulk Flt3L-DCs or were stained with antibodies against CD11c and B220 and sorted by FACS using FACSVantage SE (with DIVA upgrade). CD11clow $B220^+$ cells were used as bone marrow pDCs. The purity of pDCs was greater than 90% based on FACS analysis. To isolate BMDMs, bone marrow cells were cultured in DMEM containing 10% FBS and 10 ng/ml CSF-1 (Sigma). Twenty four hours later, non-adherent cells were transferred to a new flask and cultured for 3 days before fresh media containing CSF-1 was added and cells were cultured for another 4 days. Mature macrophages were harvested by collagenase (Roche) digestion and cultured on 96-well plates for experiments. HEp-2 cells were cultured in Eagle Minimal Essential Medium (EMEM) supplemented with L-glutamine, HEPES,

penicillin, streptomycin, and 10% FBS. EL4 cells were cultured in RPMI supplemented with penicillin, streptomycin, and 10% FBS.

Antibodies

Anti-CD16/32, FITC-conjugated antibodies against CD11c, IFN-γ and I-A/E, PE-conjugated antibodies against B220, CD3, CD80 and CD86, APC-conjugated antibodies against CD11c, CD8 and B220, and PE-Cy5-conjugated anti-F4/80 were purchased from BD Pharmingen. Biotin-conjugated anti-CD2 was from BioLegend. Streptavidin-conjugated PacificBlue was from Invitrogen. Immunohistochemistry of lung samples was performed using goat anti-RSV (Biodesign) followed by rabbit anti-goat (Abcam) and detection using a Basic DAB detection kit (Ventana Medical Systems, Inc.).

Pulmonary function

Unrestrained whole-body plethysmography (Buxco Electronics) was used to monitor the respiratory function. Enhanced pause (Penh), which reflects pulmonary airflow resistance, was used to monitor the severity of clinical respiratory disease in mice.

Sample collection, histology, virus titration and cytokine measurements

Mice were anesthetized with ketamine (75mg/kg) and acepromazine (5mg/kg) before they were sacrificed by exsanguination. BALF was obtained by injecting 0.5 ml of 10% EMEM through a 25-gauge needle into the lungs via the trachea, followed by aspiration of this fluid into a syringe. For histological analysis, lungs were fixed with formalin, embedded in paraffin, sectioned, and stained with hematoxylin-eosin or with anti-RSV antibodies for immuno-histochemical analysis. For RNA measurements, lungs were perfused with 5 ml of PBS and then submerged in 2 ml of RNAlater (Qiagen). Samples were stored at 4^{o}C overnight then transferred to -20^{o}C until RNA was extracted. For T cell assays, lungs were perfused with 5 ml of PBS, then extracted and mechanically minced followed by collagenase A (1mg/ml in PBS, Roche) digestion for 30 minutes. Cells were passed through a 100 μm filter and spun down followed by erythrocyte lysis using BD PharM Lyse. Cells were then mixed with an equal volume of 40% Percol (Sigma) in PBS and spun for 20 minutes. Mediastinal lymph nodes were extracted and similarly stored in 0.5 ml of RNAlater before RNA extraction and real-time PCR analysis.

RNA extraction, microarray and quantitative PCR

To extract RNA, tissues were first homogenized and lysed in 1 ml of Trizol (Invitrogen). Lysate was mixed with Chloroform and the aqueous phase was applied to RNeasy columns (Qiagen). Subsequent steps followed the manufacture's recommended protocol and RNA integrity was assessed by using an Agilent 2100 Bioanalyzer (Agilent, Palo Alto, CA). Microarray was performed using Illumina Sentrix Mouse 6 BeadChips which were scanned on an Illumina BeadStation 500. Illumina's Beadstudio software was used to assess fluorescent hybridization signals. For each genotype, RNA from two mock treated and three RSV-infected mice was subjected to parallel microarray experiments. The iScript cDNA synthesis kit (BioRad) was used to create cDNA from 1μg of RNA. qPCR was performed with 15 ng of cDNA using Sybr Green on a BioRad iCycler with the following primers: *Ifn-β* (TCCGAGCAGAGATCTTCAGGAA; TGCAACCACCACTCATTCTGAG), IL-6 (TCCATCCAGTTGCCTTCTTG; GGTCTGTTGGGAGTGGTATC), *Tnf-α* (CCTCCCTCTCATCAGTTCTATGG; GGCTACAGGCTTGTCACTCG), *Il-1β* (TCTATACCTGTCCTGTGTAATG; GCTTGTGCTCTGCTTGTG), *Cxcl-16* (AGCGCAAAGAGTGTGGAACT; GGTTGGGTGTGCTCTTTGTT), *Il-24* (CCCTGCCTGAGCCTAATC; CAAGACCCAAATCGGAACTC), *Actin* (TGACGTTGACATCCGTAAAGACC; AAGGGTGTAAAACGCAGCTCA).

Western blotting

Lungs were lysed in Tris-buffered saline with 0.2% NP40, protease inhibitor cocktail (Roche), DTT (1mM), and PMSF (0.2 mM). Samples were homogenized and centrifuged at 17,500 x g in a tabletop centrifuge. Protein content was measured in supernatants and 20μg of protein from each sample was subjected to SDS-PAGE followed by western blotting with antibodies against β-actin (Cell Signaling), phospho-STAT-1 (Cell Signaling), and STAT-1 (Santa Cruz Biotech.).

Statistics

For microarray data analysis, normalization of signal values per chip and per gene was achieved using the gene expression analysis software program, GeneSpring, Version GX 7.2.3 (Agilent). Analysis was restricted to probe sets for which a P (present) call was obtained in at least one of the sample genotype evaluated (quality control probes). Welch t-test ($p<0.01$) followed by a 2 fold change filter was used to rank genes on the basis of their ability to discriminate between pre-defined genotypes. Only mock-treated mice of the WT-group are displayed in the figures as all mock treated mice displayed very similar gene expression levels. Other comparisons were made using a one way analysis of variance (ANOVA)

with a Tukey's test when the ANOVA result indicated a significant difference ($p<0.05$).

Results

In the first series of experiments, we studied the cell-specific IFN-I response to RSV. Lung fibroblasts, bone marrow-derived macrophages (BMDM) and conventional dendritic cells (cDC) were isolated and infected with RSV. Measurement of IFN-α and IFN-β production by ELISA, shown in Fig. 3 (A-E), revealed that IFN-I induction by RSV in all of these cell types was completely dependent on MAVS. Previous studies have suggested that plasmacytoid DCs (pDCs) rely on TLR7 and MyD88 to induce IFN-I in response to RNA viruses, while other cell types employ the RLR-MAVS pathway. Although Sendai virus (SeV) infection triggered IFN-I production in purified pDC, we were unable to detect any IFN-α or IFN-β in these cells following RSV infection (Fig. 4A). Consistent with this result, the induction of IFN-α and IFN-β by RSV was dependent on MAVS in bone marrow cells treated with Flt3 ligand, which leads to the generation of pDC and cDC (Fig. 4, B & C). In contrast, infection of Flt3L-DCs with SeV triggered IFN-I production in a manner that was independent of MAVS. This is consistent with our previous finding that MAVS is dispensable for

IFN-I induction by SeV in pDC, which is the major source of IFN-I in SeV-infected Flt3L-DC.

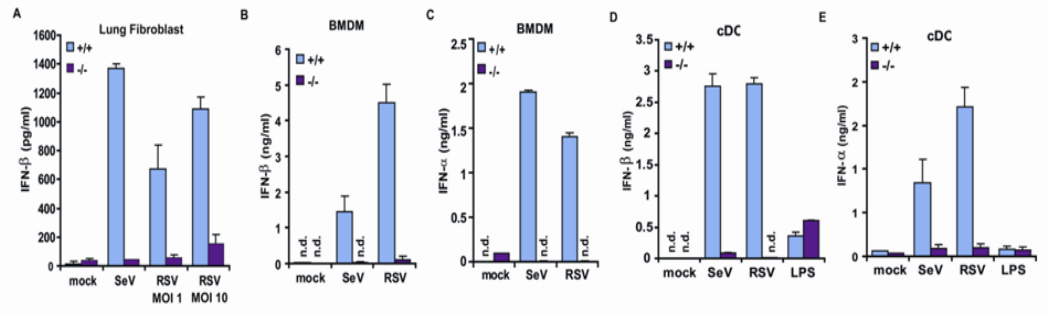

Figure 3. In vitro cytokine responses to RSV infection are lost in the absence of MAVS. Adult lung fibroblasts (**A**), bone-marrow-derived macrophages (BMDM; **B**, **C**), cDCs (**D**, **E**) from wild-type(+/+) and *Mavs*$^{-/-}$(-/-) mice were infected with SeV or RSV for 24 hours before culture supernatants were analyzed for IFN-β or IFN-α, by ELISA. Data are represented as mean +/- SD.

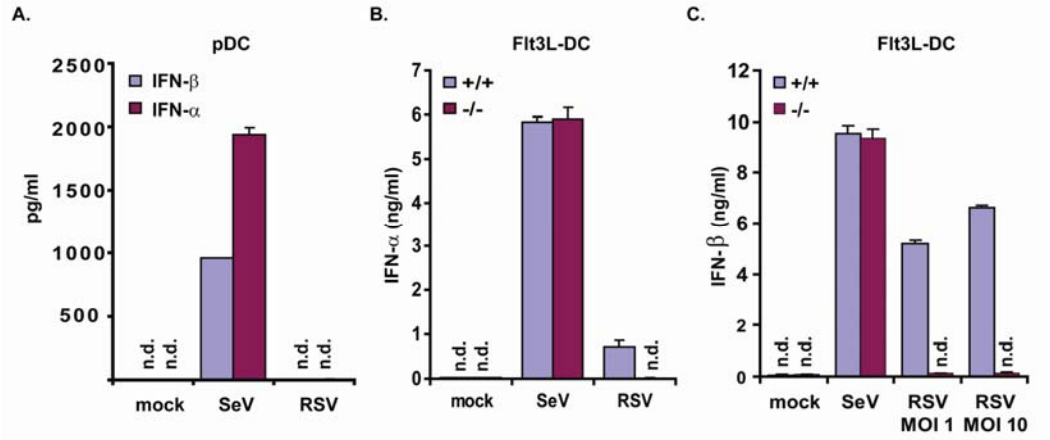

Figure 4. IFN-I response in pDC in vitro. (**A**) Purified, wild-type, pDC from Flt3L stimulated bone-marrow cultures were mock infected or infected with SeV (50 HA U/ml) or RSV (MOI=1) for 24 hours. Supernatants were then tested for IFN-β and IFN-α by ELISA. (**B, C**) Bulk Flt3L stimulated bone marrow cultures were mock infected or infected with SeV (50 HA U/ml) or RSV (MOI = 1 or 10 as indicated) for 24 hours. Supernatants were then tested for IFN-α (**B**) and IFN-β (**C**) by ELISA. n.d.: not detected.

To examine the role of MAVS and MyD88 in RSV infection in vivo, we infected *Mavs*$^{-/-}$, *Myd88*$^{-/-}$ and DKO mice with RSV via the intranasal route (Fig. 5). Consistent with the in vitro results, one day after infection, wild-type mice secreted large amounts of IFN-I which were detected in bronchoalveolar lavage fluid (BALF). This response was normal in MyD88-null mice but completely abolished in mice lacking MAVS. Consistently, MAVS-deficient mice failed to induce and activate STAT1 in the lung following RSV infection, whereas this interferon signaling response was normal when these mice were infected with Vesicular Stomatitis Virus (VSV), an RNA virus known to induce IFN-I independent of MAVS [Fig. 6; (Sun, Sun et al. 2006)]. Other pro-inflammatory cytokines, including IL-6, TNF-α, MCP-1, and IL-1β also depended on MAVS for their expression. Interestingly, maximal production of TNF-α, MCP-1 and IL-1β also required MyD88. At the same time point, day 1, we were unable to detect significant levels of IFN-γ, IL-12, or IL-10 in the BALF (data not shown). Neither IFN-α nor IFN-β was detectable in sera and mediastinal lymph nodes by ELISA or quantitative PCR in mice of any genotype (data not shown). Recently, it has been shown that, in response to intranasal Newcastle Disease Virus infection, IFN-α-producing alveolar macrophages and cDC could be detected after 24 hours in wild-type mice (Kumagai, Takeuchi et al. 2007). In MAVS-deficient animals, however, this response was abolished and a compensatory IFN-α response was detected in pDCs at 48 hours. However, we found no evidence of IFN-I

production 2, 5, 9, or 14 days after RSV infection in *Mavs*$^{-/-}$ mice (Fig. 7 and data not shown), consistent with our in vitro observation that RSV does not induce IFN-I in pDC.

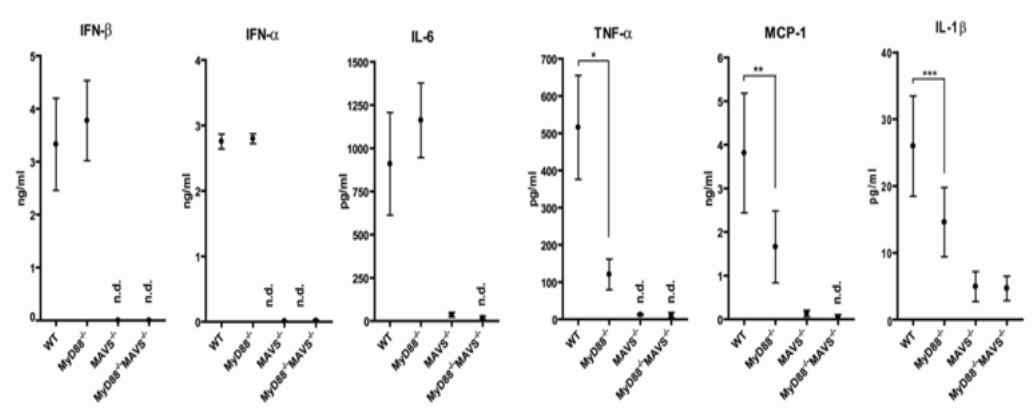

Figure 5. In vivo cytokine responses to RSV infection are lost in the absence of MAVS. Mice of the indicated genotypes were intranasally infected with RSV (10^7 PFU) for 24 hours and then bronchoalveolar lavage fluid (BALF) was harvested for cytokine measurements by ELISA (for IFN-α, IFN-β and IL-1β) or Cytometric Bead Array (CBA; for IL-6, TNFα and MCP-1) (*, $p < 0.001$; **, $p < 0.01$; ***, $p < 0.05$; ANOVA, Tukey's Test) (n=4 per group). n.d.: not detected. Data are represented as mean +/- SEM.

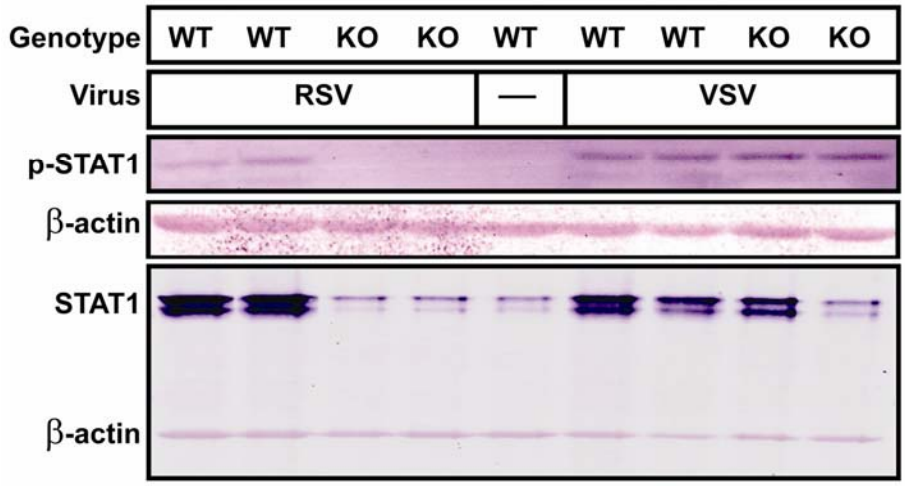

Figure 6. STAT-1 induction and activation in the lung following viral infection. Wild-type and *Mavs*$^{-/-}$ mice were mock infected (lane 5), or infected with RSV (4 mice; lanes 1-4) or VSV(4 mice, lanes 6-9) intranasally for 24 hours. Lung homogenates were analyzed by Western blotting using antibodies against p-STAT1, STAT1 or β-actin.

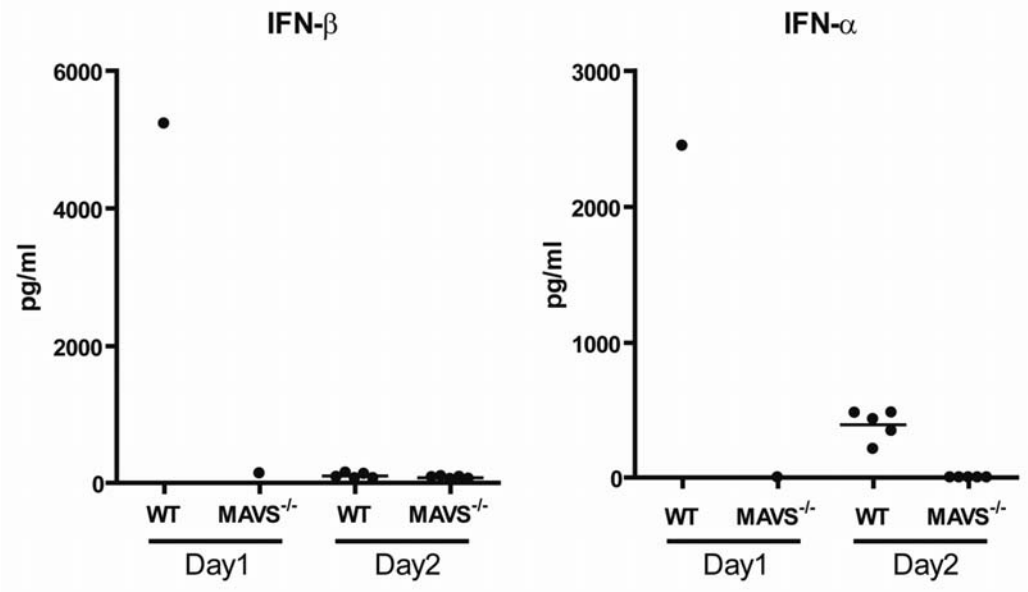

Figure 7. Type-1 IFN production after in vivo RSV infection. Wild-type and *Mavs*$^{-/-}$ mice were infected with RSV for 24 or 48 hours and then BALFs were extracted for measurements of IFN-β (**A**) and IFN-α (**B**) by ELISA.

To evaluate the roles of MyD88- and MAVS-mediated signaling in the global pulmonary innate immune response to RSV, we analyzed lung RNA by microarray 24 hours after infection (Fig. 8). Of the 659 genes induced by 2-fold or more in wild-type mice, 440 (~66.8%) were dependent on MAVS but not MyD88, 12 (~1.8%) were dependent on MyD88 but not MAVS, and 90 (13.7%) were dependent on both (Fig. 8A). The induction of most interferon-related genes was MAVS-dependent and MyD88-independent (Fig. 8B). A similar pattern of dependence was seen for most of the cytokine-, chemokine-, and PRR-related genes (Fig. 8C-E and Fig. 9). In contrast, optimal expression of TNF-α and IL-1β was dependent on both adaptors (Fig. 8F). Interestingly, both IL-24 and Cxcl-16

were induced in all RSV-infected groups compared to mock treated groups. With the exception of these chemokines, innate immune responses were largely absent in *Mavs*$^{-/-}$ and DKO mice.

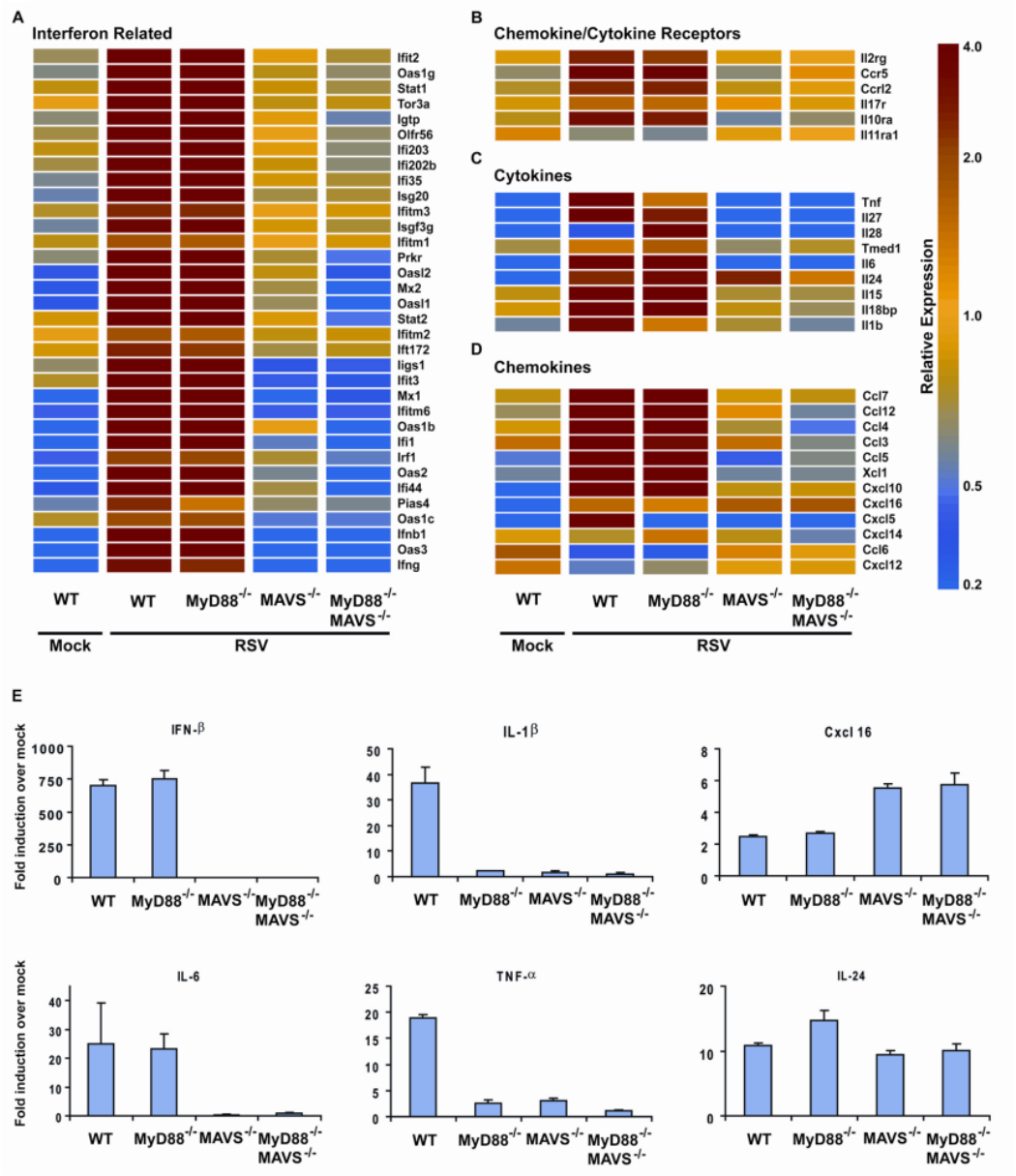

Figure 8. Global gene expression analysis of lung RNA after infection with RSV reveals profound defects in mice lacking MAVS. For each genotype, two mice were mock treated and three were inoculated with RSV (10^7 PFU) for 24 hours before lungs were harvested for total RNA extraction, which was analyzed by microarray. (**A-D**) Mean relative expression of genes known to be involved in immune responses, including interferon-related (**A**), chemokine or cytokine

receptors (**B**), cytokines (**C**), and chemokines (**D**). (**E**) Induction of selected genes was confirmed by qPCR. Data are represented as mean +/- SEM.

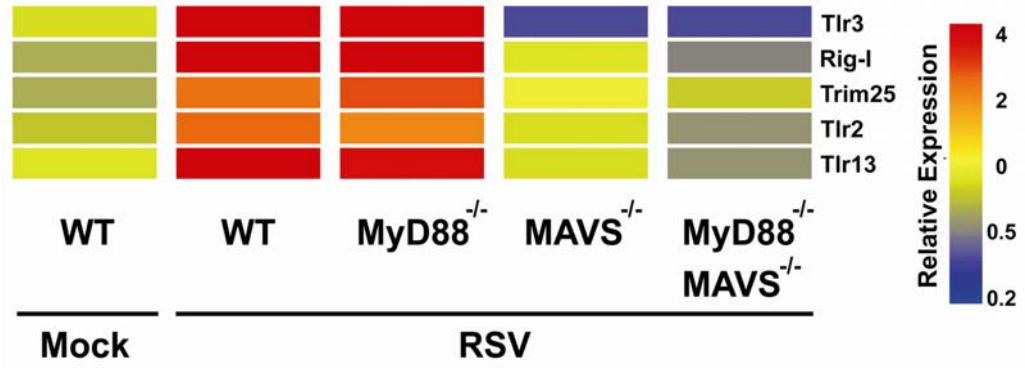

Figure 9. Microarray analysis of pattern recognition receptor (PRR)-related genes. Mean relative expression of PRR-related genes from the experiment shown in Figure 2 that met t-test and the expression filter requirements are shown for the indicated mock and RSV-treated groups.

Next, we evaluated viral clearance in these mice by measuring viral loads in the BALF at various times after infection. In wild-type mice, viral loads peaked on day 5 after infection and reached undetectable levels by day 9 as previously observed in this model (Fig. 10A). Consistent with a previous study, MyD88-deficient mice showed no significant differences in viral clearance compared to wild-type mice. In contrast, viral loads in *Mavs*$^{-/-}$ mice were about 100 times higher than those in the wild-type mice on day 1 and 5 post infection. Surprisingly, despite the absence of IFN-I and other antiviral molecules, these mice were able to clear the virus to undetectable levels by day 9. The DKO mice showed no significant difference in viral loads compared to the *Mavs*$^{-/-}$ group one day after infection, suggesting the importance of MAVS- but not MyD88-mediated viral clearance in the early phase of infection. This is consistent with the lack of a pDC response which would otherwise be the major source of early TLR-dependent antiviral interferons. As the infection progressed, however, DKO mice harbored significantly higher viral loads compared to all other genotypes. Remarkably, DKO mice were also able to clear the infection by day 28 (Fig. 10B).

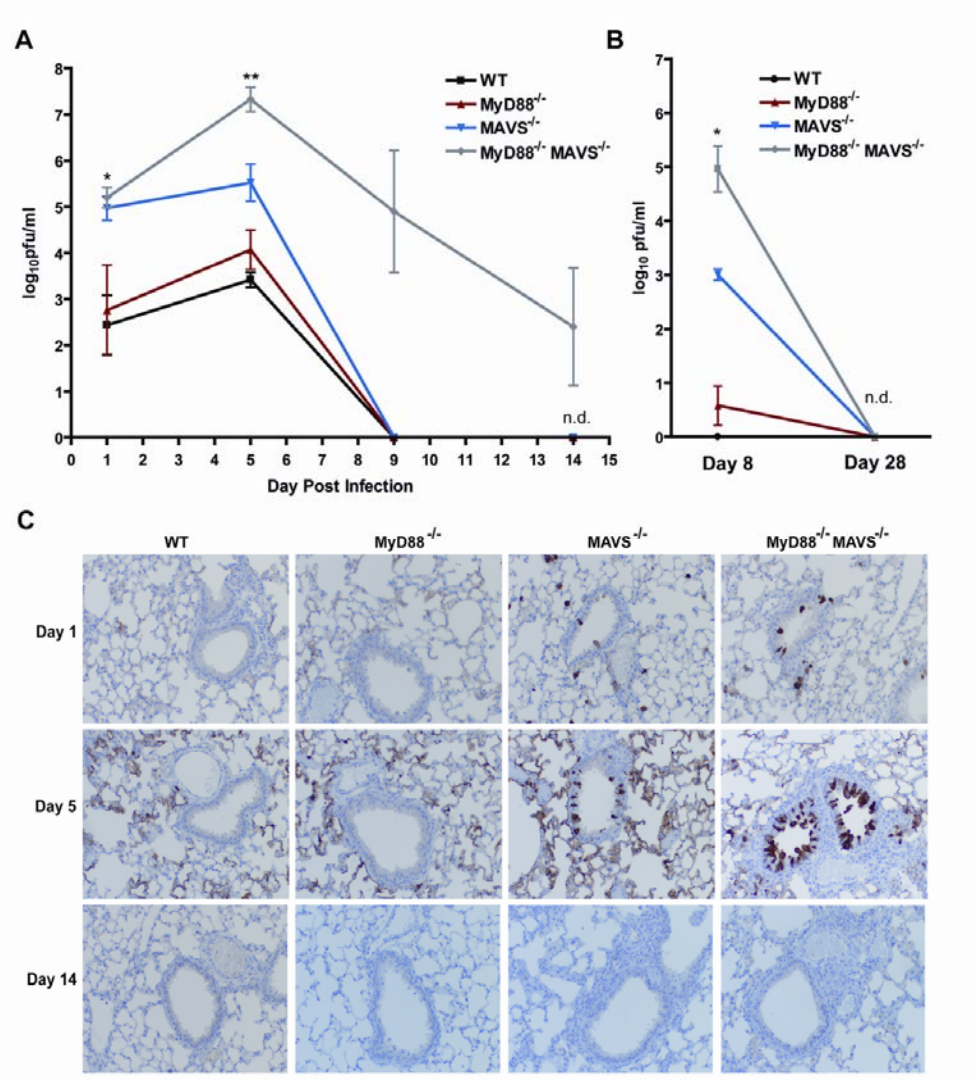

Figure 10. *Mavs*$^{-/-}$ and DKO mice are able to clear RSV. (**A, B**) Wildtype, *Myd88*$^{-/-}$, *Mavs*$^{-/-}$ and *Myd88*$^{-/-}$*Mavs*$^{-/-}$ mice were infected with RSV (10^7 PFU) and bronchoalveolar lavage fluid was harvested at the indicated times to measure viral loads by plaque assay. (A, *, *Mavs*$^{-/-}$ vs. *Myd88*$^{-/-}$ $p < 0.001$; **, *Mavs*$^{-/-}$ vs. DKO and *Mavs*$^{-/-}$ vs. *Myd88*$^{-/-}$ $p < 0.001$; B, *, *Mavs*$^{-/-}$ vs. DKO and *Mavs*$^{-/-}$ vs. *Myd88*$^{-/-}$ $p < 0.01$; ANOVA) (n=3-5). (**C**) Lungs from infected mice and mock controls were analyzed by immuno-histochemistry using a polyclonal anti-RSV antibody.

Consistent with unrestricted viral replication in *Mavs*$^{-/-}$ and DKO mice in the early phase of RSV infection, immuno-histochemical staining with RSV antibodies in the lungs of these mice showed evidence of infection of ciliated respiratory epithelium lining the bronchioles and bronchi on day 1 and day 5 after infection (Fig. 10C). This staining was undetectable by day 14. Histological examination of lungs of infected mice revealed no striking differences on day 1 (Fig. 11A). On day 5, the inflammation seen in DKO mice appeared in patches compared to the diffuse inflammation in the other three genotypes. At this time point, there was no gross difference in the composition of the cellular infiltrate among all groups. However, few multinucleated syncytial cells were observed in the bronchioles of DKO mice (Fig. 11B). On day 14, inflammation had largely subsided in WT and *Myd88*$^{-/-}$ mice but remained in the other two groups. Although *Mavs*$^{-/-}$ mice had some chronic inflammation at this stage, DKO mice exhibited patchy acute pneumonia, numerous syncytial cells and reactive bronchial epithelium (Fig. 11C). By day 28, inflammation was significantly reduced and comparable in all genotypes (Fig. 11D).

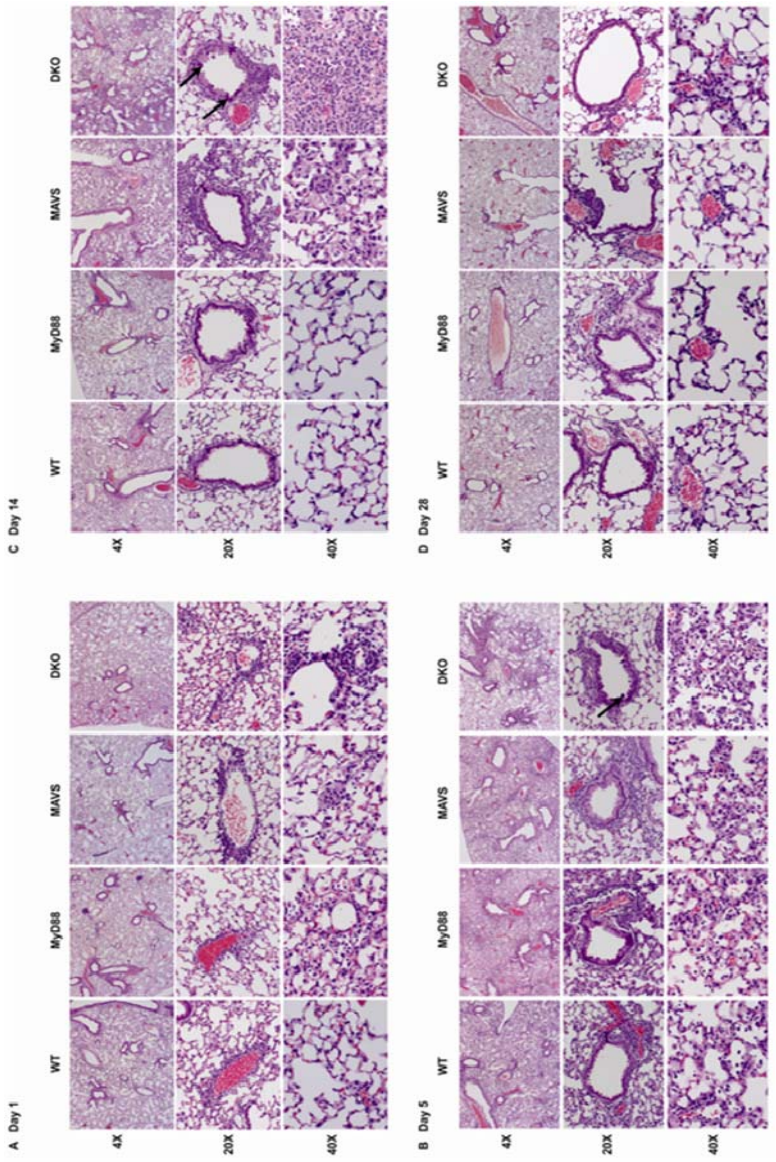

Figure 11. Pulmonary histopathology. Wild-type, *Myd88*$^{-/-}$, *Mavs*$^{-/-}$, and DKO mice were infected with RSV for 1 (**A**), 5 (**B**), 14 (**C**), or 28 (**D**) day(s) before lungs were removed for staining with hematoxylin-eosin. Representative sections at the indicated magnifications are shown for each genotype. Arrows indicate multinucleated syncytia.

Next, we evaluated the roles of MAVS and MyD88 signaling in the pulmonary function of mice by plethysmography (Fig. 12). One day after infection, only wild-type mice exhibited pulmonary dysfunction, possibly due to inflammatory cytokine responses that cause airway obstruction ($p<0.0001$). We also consistently noted that only wild-type mice had ruffled hair and were less active than other genotypes on day one. This is consistent with cytokine measurements, which showed that mice lacking MAVS, MyD88, or both, had markedly reduced levels of the pro-inflammatory cytokines TNFα, IL-6 and IL-1β (Fig. 5 & 8). Between day 2 and 10, all groups developed increased airway obstruction compared to their baseline function. Whereas the wild-type, *Mavs*$^{-/-}$ and *Myd88*$^{-/-}$ mice returned to normal function around day 10, the DKO mice experienced slightly prolonged pulmonary dysfunction but eventually also returned to normal lung function (Fig. 12; day 12, $p=0.03$; day 14, $p=0.04$).

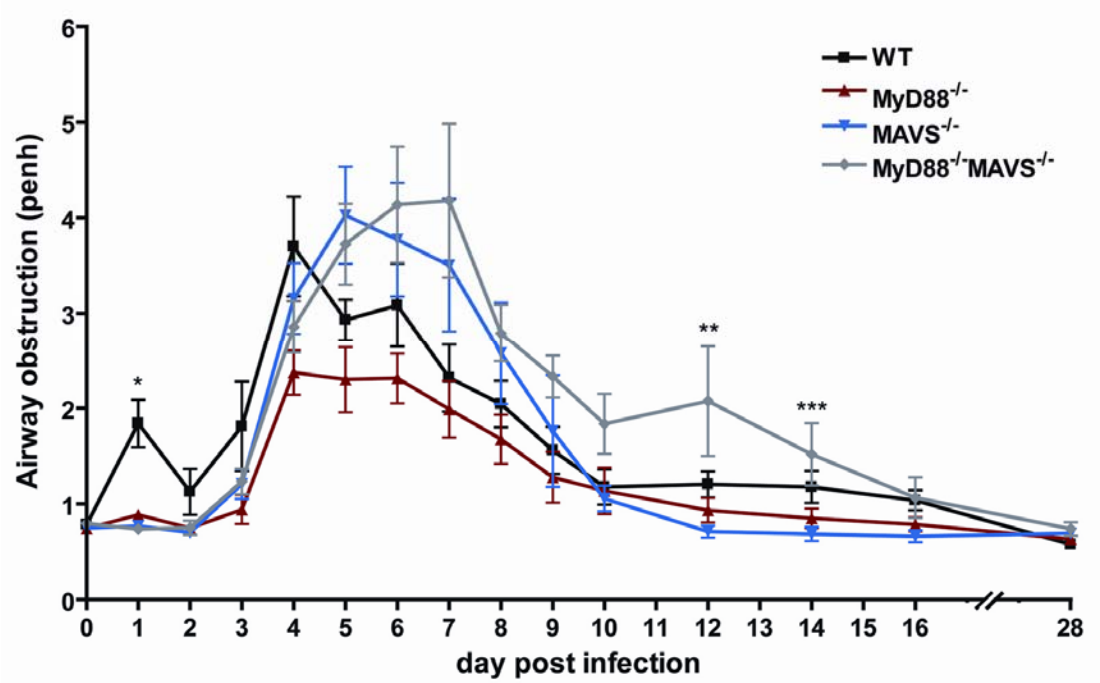

Figure 12. *Mavs*$^{-/-}$ and DKO mice are able to resolve pulmonary disease. Mice infected with RSV were assessed by whole-body plethysmography to measure airway obstruction (*, $p < 0.0001$; **, $p < 0.03$; ***, $p < 0.04$; ANOVA). n.d.: not detected. Data are represented as mean +/- SEM.

Conclusions

These data provide both in vivo and in vitro evidence that MAVS is essential for the production of IFN-I, inflammatory cytokines and chemokines in response to RSV infection. As expected and consistent with data using a variety of RNA-viruses, non-pDC depend entirely on the RLR pathway for innate response to infection. Our result that in vitro generated pDC do not produce IFN-I in response to RSV is surprising but consistent with the lack of IFN-I production in vivo in mice lacking MAVS. Published data reveals a confusing picture of the role of these cells in anti-RSV immunity. It has been shown that IFN-I responses are not elicited in human pDC infected with RSV-A2, the same strain used in our study (Schlender, Hornung et al. 2005). That study found that prior infection with RSV inhibited IFN-I induction by TLR7 and TLR9 ligands, suggesting active immune evasion by the virus. There are conflicting reports of the role pDCs play in response to RSV infection in vivo with some suggesting no role in IFN-I secretion and others showing the opposite (Wang, Peters et al. 2006; Boogaard, van Oosten et al. 2007; Jewell, Vaghefi et al. 2007). The reasons for such mixed results are unclear and may be partly explained by differences in host species, in viral dose, or in methods used to generate, isolate or deplete pDC. Analysis of primary pDC from IFN-α-GFP and IFN-β-GFP reporter mice infected with RSV will help address this issue.

Global gene expression profiling further demonstrated that MAVS is required for RSV-induced production of the vast majority of antiviral molecules. In contrast to MAVS, MyD88 is dispensable for the induction of IFN-I and the majority of antiviral cytokines with a few exceptions such as TNF-α, IL-1β, and MCP-1. The defective production of these molecules in all of the mutant mice may reflect the complex regulation unique to these potent inflammatory mediators. Notably, *Il-24* and *Cxcl-16* were induced independently of MAVS and MyD88. Whether these cytokines play any role in the immune response to RSV requires further study.

It has recently been shown that systemic infection with the RNA virus, LCMV, results in IFN-I and inflammatory cytokine and chemokine production in a MyD88-dependent but largely MAVS-independent manner (Jung, Kato et al. 2007). Using an intranasal mode of infection, the same group found that influenza virus induction of IFN-I is defective only in mice lacking both MAVS and MyD88 (Shohei Koyama 2007). Further, pulmonary NDV infection indicated that mice lacking either MAVS or MyD88 are still capable of producing IFN-α (Kumagai, Takeuchi et al. 2007). These results indicate that the requirement of MAVS and MyD88 for innate cytokine responses depends on the pathogen as well as the route of infection. Our data suggest that RSV solely relies on the RLR-MAVS pathway for IFN-I induction in vivo. Our observation that RSV-infected

Myd88$^{-/-}$ mice induce normal levels of IFN-I, suggests that, in this model, pDC do not produce these cytokines as they are expected to utilize TLR7 which requires MyD88 for signaling.

Despite such a drastically defective cytokine response and the fact that *Mavs*$^{-/-}$ mice harbored higher viral loads shortly after RSV infection, these mice still cleared the virus effectively. While deletion of *Myd88* alone had no effect on RSV loads, mice lacking both adaptors had higher and more prolonged viral loads than those lacking either one alone, suggesting that in the absence of MAVS, MyD88 signaling contributed to antiviral immunity through a mechanism independent of IFN-I induction. Notably, DKO mice harbored similar viral loads compared to *Mavs*$^{-/-}$ mice one day after infection suggesting that early control of viral replication is mediated solely and non-redundantly by MAVS.

CHAPTER THREE

MAVS AND MYD88 IN ANTI-RSV ADAPTIVE IMMUNITY

Introduction

The adaptive immune response plays a pivotal role in the clearance of RSV. In the mouse model of RSV infection, both B and T cells are robustly recruited to the lung after infection. The requirement of these cells for normal clearance of the virus has been shown by antibody-mediated depletion experiments. Graham et al used anti-CD4 (GK1.5) and anti-CD8 (2.43) antibodies to deplete the respective T cell populations in mice and found that both cell types are required for normal clearance of RSV (Graham, Bunton et al. 1991). Mice depleted of both populations failed to develop RSV-induced sickness compared to WT counterparts, indicating that the T cell response contributes to the disease rather than direct viral effects. $CD8^+$ T cells were found to be the major contributor to illness.

As discussed earlier, PAMP recognition by DCs is thought to be crucial for productive activation of adaptive T cells. The roles of MyD88 and TLR3 have been tested in the mouse anti-RSV immune response. Although deletion of either gene had no impact on the kinetics of viral clearance, mice lacking either

molecule were found to develop a more Th2-skewed response compared to WT mice (Rudd, Smit et al. 2006; Rudd, Schaller et al. 2007). Upon anti-CD3 and anti-CD28 stimulation, TLR3-deficient lymph node cells taken from RSV infected mice produced more IL-5 and IL-13 than WT cells. In addition to up-regulated production of these Th2 cytokines, lymph node cells taken from RSV infected *Myd88*$^{-/-}$ mice produced more IL-4 and less IFN-γ compared to WT cells. In both groups of mutant mice, the Th2 shift correlated with increased mucus production in the airways and increased eosinophilia.

In terms of DCs, *Myd88*-deficiency had little effect on RSV-induced upregulation of MHC-II and the co-stimulatory molecules, CD40 and CD80 (Rudd, Schaller et al. 2007). However, MyD88 was absolutely required for IL-12 p70 secretion by BMDCs upon infection with RSV. Together, these data indicate that TLRs do play some role in T cell function in response to RSV. However, to my knowledge, there are no studies that examine the role of TLRs or other PRR components on RSV induced specific $CD4^+$ and $CD8^+$ T cell activation.

Both humans and mice produce neutralizing antibodies to RSV (Domachowske and Rosenberg 1999). However, antibody titers in both species decline rapidly following viral clearance and this may partially explain the poor development of immune memory to the virus. In mice, antibodies seem not to play a major role in

viral clearance during primary RSV infection (Graham, Bunton et al. 1991). Interestingly, although anti-μ mediated B cell depletion had no effect on viral titer following infection of naïve mice, it did exacerbate disease and lung pathology. B cell responses are required for normal viral clearance during rechallenge in the mouse model. That depletion of $CD4^+$ T cells abrogated anti-RSV antibody production indicates that this is a T-dependent response and such B cell responses are thought to depend on TLR activation (Graham, Bunton et al. 1991; Pasare and Medzhitov 2005). However, this has not been investigated in the case of RSV infection.

We were surprised by the fact that DKO mice are able to clear RSV given the lack of an innate IFN-I or pro-inflammatory cytokine response, which are considered important for adaptive activation and which, by themselves, limit viral replication. Thus, we decided to assess the adaptive immune activation in the infected mice.

Hypotheses and Aims

The clearance of RSV and resolution of disease in DKO mice lead us to hypothesize that, despite a drastically deficient innate response, these mice are

able to activate an effector arm of the adaptive immune system which then mediates viral clearance.

Our aims to test this hypothesis were to:

1. Measure anti-RSV antibody titers after RSV infection to assess B cell activation
2. Measure CTL IFN-γ production and specific killing to assess the activation of these cells.

Material and Methods

RSV antibody measurements

For measurement of RSV-specific antibody levels, blood was collected by tail vein bleeding or by cardiac puncture at the time of sacrifice. Samples were spun at 9,600 x g in a microcentrifuge for 10 minutes and the sera were separated and stored at 80^{o}C until analysis. To make RSV-coated ELISA plates, HEp-2 cells were infected with RSV for 48 hours and then culture supernatants were diluted 1:20 in carbonate coating buffer (150mM sodium carbonate, 350mM sodium bicarbonate, pH 9.6). 100 µl of the diluted supernatants was applied to each well

of a 96-well ELISA plate followed by overnight incubation at 4^{o}C. Antigen negative wells were coated with diluted supernatants from sterile HEp-2 cultures. The performance of the ELISA plates was tested for specificity using sera from uninfected mice. Additionally serum dilution curves were generated using serum from wild-type mice infected with RSV. A dilution of 1:200 was subsequently used for all samples to achieve optimal sensitivity in the linear range of the assay. ELISA was performed using HRP-conjugated goat anti-mouse IgG (Santa Cruz Biotech), biotinylated goat anti-mouse IgG1 and biotinylated goat anti-mouse IgG2a (Zymed). Streptavidin-HRP was from R&D systems.

$CD8^{+}$ T cell analyses

For interferon gamma production, lung cells were incubated in complete media with either a SeV-derived peptide (FAPGNYPAL) or an RSV-derived peptide (NAITNAKII) (10 μg/ml) and brefeldin A (10 μg/ml, Sigma) for 6 hours (Rutigliano, Rock et al. 2005). Cells were then incubated with antibodies against CD3 and CD8 followed by fixation, permeabilization and staining for IFN-γ using the BD fix/perm reagent according to the manufacturer's instructions. Samples were run on a BD FACSCaliber and analyzed using FlowJo 8.3 (Tree Star Inc.). Cytotoxicity assays were performed as previously described. Briefly, EL4 targets were incubated with either RSV- or SeV-derived peptides (10ug/ml) overnight.

RSV-peptide loaded targets were then labeled with 5μM carboxyfluorescein succinimidyl ester (CFSE) and control targets with 0.5μM CFSE before mixing them at a 1:1 ratio. Mixed targets were then incubated at the indicated effector:target (E:T) ratios with lung cells from mice infected with RSV for 8 days. Cells were incubated at 37^{o}C for 4 hours and then were analyzed by flow cytometry. Percent specific lysis was calculated as 100-(100 x percent $CFSE^{high}$ (at E:T of 2 or 20) / percent $CFSE^{high}$ (at 0:1)).

$CD8^{+}$ T cell depletion

Mice were intra-peritoneally injected with 200μg of purified 2.43 antibody or control rat IgG in PBS on days -2, 0, 2, 4, and 7 during the course of RSV infection.

Dendritic cell analysis

For in vitro assessment of DC activation, 7-day GM-CSF matured bone marrow cells were treated with LPS (1ug/ml), RSV (MOI = 1), or SeV (50 HA U/ml) for 24 hours. Cells were then blocked with anti-CD16/32 and incubated with antibodies against CD11c and CD86 before analysis using a BD FACSCalibur.

For in vivo DC analysis, mice were infected with RSV. Twenty four hours later, they were sacrificed and lungs were removed and digested as described above to create single cell suspensions. Mediastinal lymph nodes were also removed and mashed between glass slides to create single cell suspensions. Cells were blocked with anti-CD16/32 and then stained before analysis on a CyAn ADP flow cytometer.

Results

The surprising ability of *Mavs*$^{-/-}$ and DKO mice to clear RSV led us to examine anti-RSV adaptive immune responses in these mice. Serum anti-RSV antibody responses, including the production of both IgG1 and IgG2a, were significantly attenuated in mice lacking either MAVS or MyD88, and were reduced even further in the DKO mice (Fig. 13). These results suggest that both MAVS and MyD88 play an important role in the generation of anti-RSV antibodies in the adaptive phase of the antiviral response. This is in contrast to antibody production in response to influenza, which is MyD88-dependent and MAVS-independent. However, depletion of B cells followed by RSV infection, has suggested that the antibody response is unlikely to be a major mediator of primary RSV clearance.

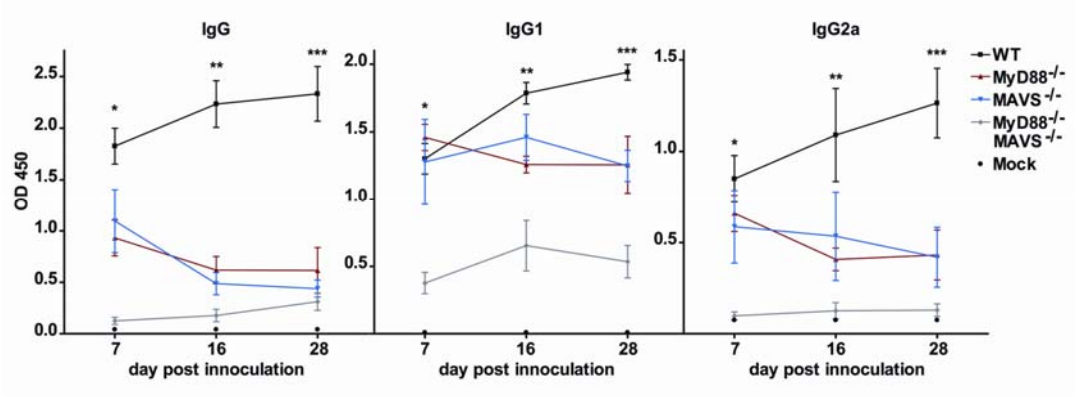

Figure 13. Antibody responses in mice lacking *Mavs* and *Myd88*. (**A**) RSV-specific antibody subtypes, IgG, IgG1 and IgG2a, were measured by ELISA using sera taken on the indicated day after RSV infection (IgG; *, WT vs. *Myd88*$^{-/-}$ $p < 0.01$, *Myd88*$^{-/-}$ vs. DKO $p < 0.05$; ** and ***, WT vs. *Myd88*$^{-/-}$ $p < 0.001$) (IgG1; *, *Mavs*$^{-/-}$ vs. DKO $p < 0.01$; ** and ***, WT vs. *Myd88*$^{-/-}$ and *Myd88*$^{-/-}$ vs. DKO $p < 0.05$) (IgG2a; *, WT vs. *Myd88*$^{-/-}$ and *Mavs*$^{-/-}$ vs. DKO $p < 0.01$; **, WT vs. *Mavs*$^{-/-}$ $p < 0.001$; ***, WT vs. *Myd88*$^{-/-}$ $p < 0.001$) (ANOVA, Tukey's Test) (n = 7–10 per group).

Next, we examined the activation of $CD8^+$ cytotoxic T lymphocyte (CTL) response in the lungs of mice following intranasal infection of RSV. Eight days after infection, lung cells were stimulated in vitro with an RSV-derived peptide previously identified as a $CD8^+$ T cell stimulating epitope or with a control SeV-derived peptide, both of which bind H2-Db. The percentage of IFN-γ – producing $CD8^+$ pulmonary T cells was quantified by FACS (Fig. 14A and B). Unexpectedly, RSV-specific $CD8^+$ T cell activation was similar in *Myd88*$^{-/-}$ and *Mavs*$^{-/-}$ mice compared to wild-type counterparts. Even the DKO mice were clearly able to activate $CD8^+$ T cells in response to RSV, although the responses were slightly, but not significantly, lower ($p=0.35$). In fact, measurement of IFN-γ in the BALF of WT and DKO mice at various times after infection revealed that DKO mice produced this cytokine more robustly than WT counterparts (Fig. 15). In WT mice, IFN-γ peaked on day 6 after RSV infection and was undetectable by day 10. In DKO mice, however, IFN-γ peaked on day 8 at a higher level than in WT mice, suggesting that the higher viral load in DKO mice led to a corresponding increase in IFN-γ production. Additionally, analysis of $CD8^+$ T cell cytolytic activity showed that, compared to cells from mock-treated animals, lung cells from RSV infected mice of all genotypes demonstrated increased ability to specifically kill target cells loaded with the MHC-I binding RSV-epitope (Fig. 16). Furthermore, depletion of $CD8^+$ T cells in conjunction with RSV infection firmly established a role for these cells. Analysis of BALF 8 days after infection

revealed that production of IFN-γ was intact in all mice treated with control IgG but absent in mice depleted of $CD8^+$ T cells, pointing to these cells as the likely source of the cytokine (Fig. 17A). Finally, measurement of viral titers in *Mavs*$^{-/-}$ and DKO mice showed much higher levels of virus when $CD8^+$ T cells were depleted (Fig. 17B). In contrast, depletion of $CD8^+$ T cells did not increase the viral titers in wild type and *Myd88*$^{-/-}$ mice, presumably because these mice still had an intact MAVS pathway to clear the virus. Together, these data clearly show that CTL activation was intact and effective in DKO mice.

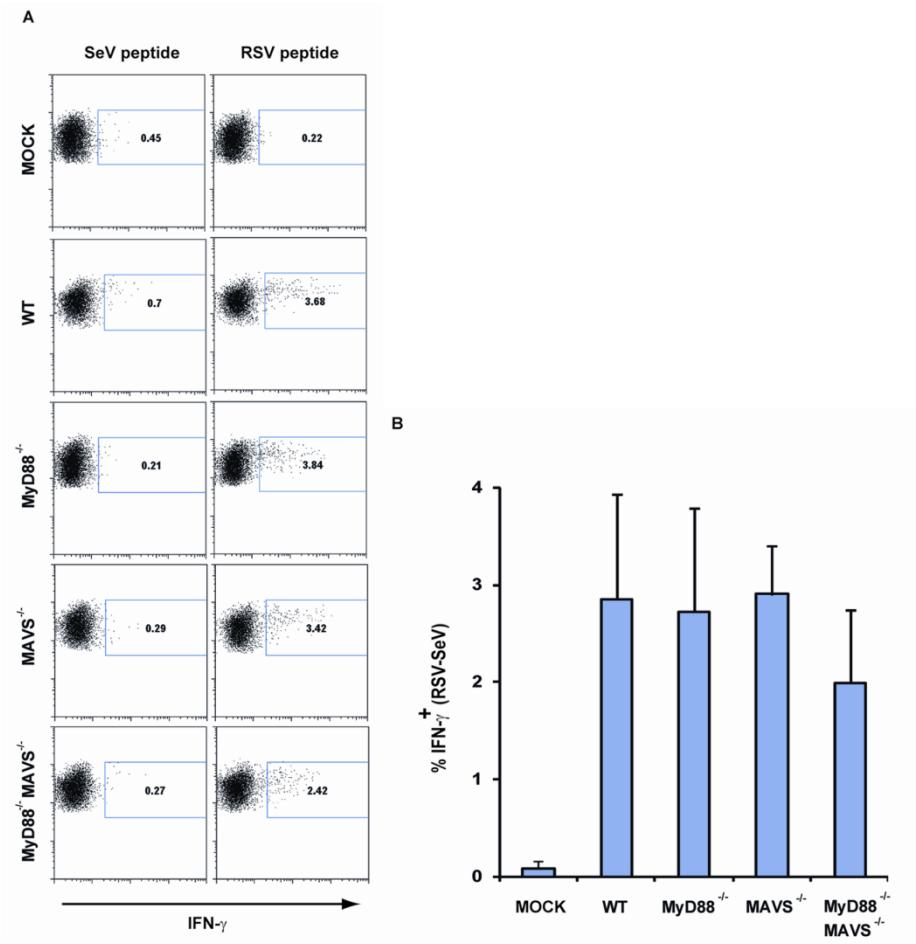

Figure 14. CD8$^+$ T cell responses in mice lacking *Mavs* and *Myd88*. (**A**) Mice were mock infected or infected with RSV for 8 days before lung cells were harvested and stimulated ex vivo with a RSV- or SeV (control) – derived peptide. Six hours after stimulation, intracellular IFN-γ levels in CD3$^+$CD8$^+$ cells were measured by FACS. The analysis of one representative mouse from each group is shown. (**B**) Data from experiments described in (**A**) are tabulated for CD3$^+$CD8$^+$ cells from all mice. The percentage of IFN-γ$^+$CD3$^+$CD8$^+$ cells in RSV-peptide treated cultures minus that from SeV-peptide cultures is plotted for each genotype ($p = 0.35$; ANOVA) ($n = 5$ per group).

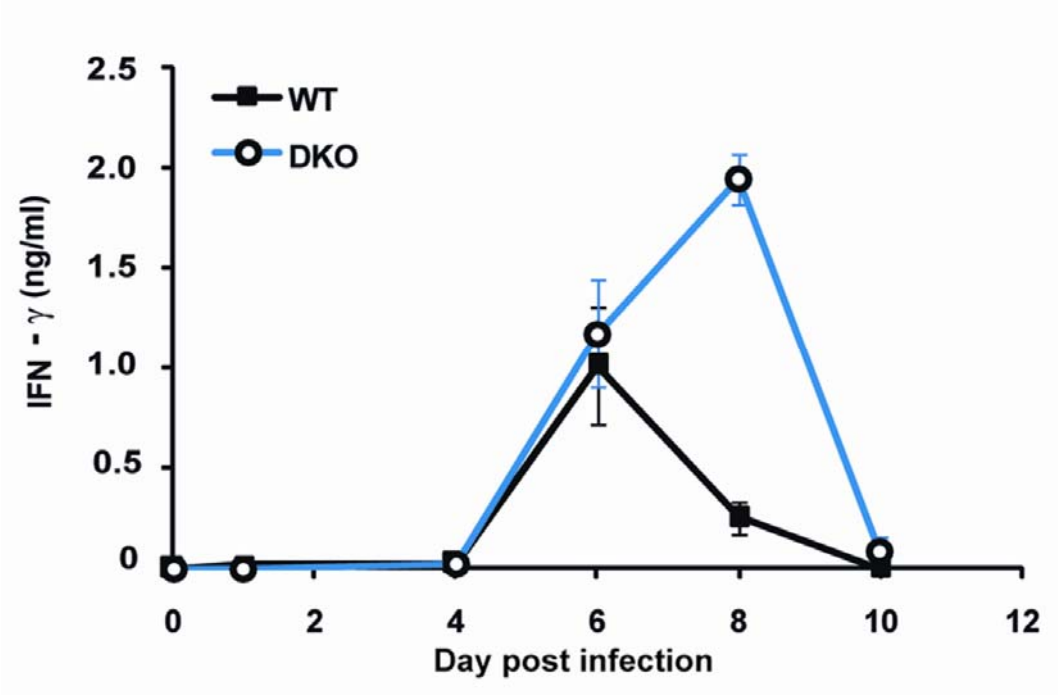

Figure 15. IFN-γ production in response to RSV. Bronchoalveolar lavage fluid IFN-γ was measured in WT and DKO mice at the indicated times after RSV infection (n = 3 per group).

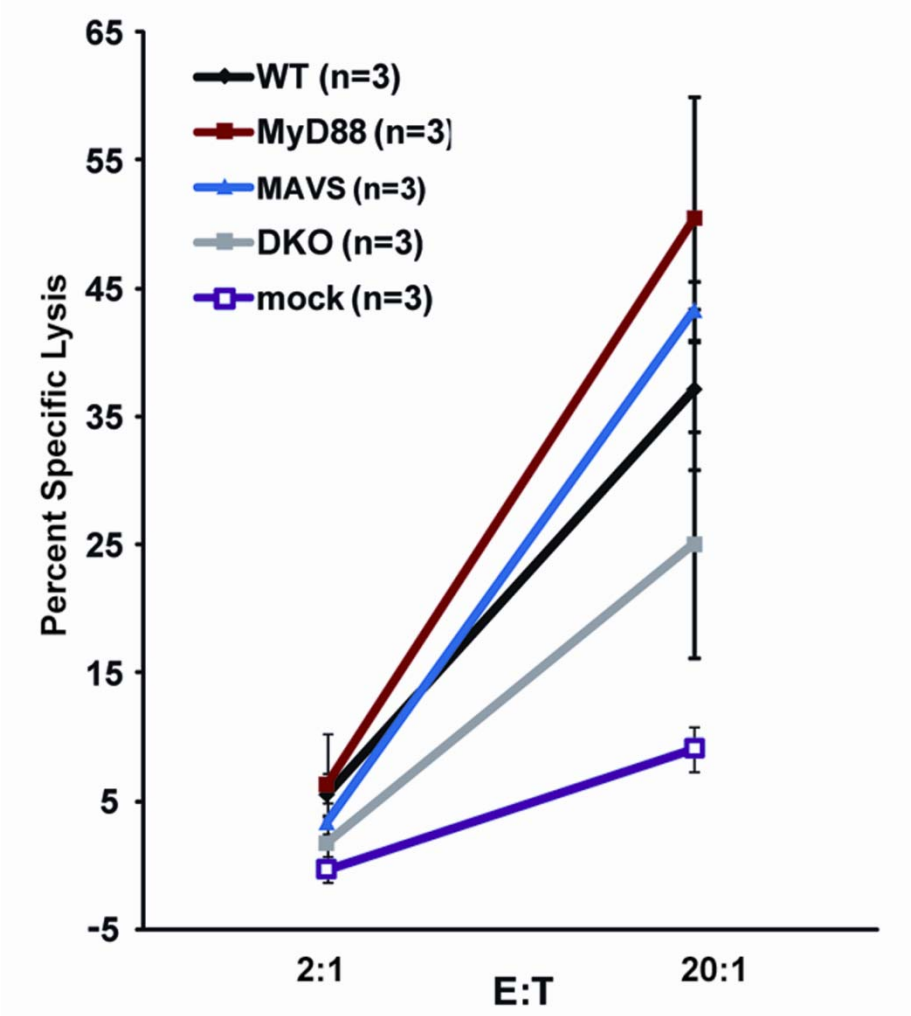

Figure 16. RSV-specific CTL cytotoxic activity . Lung cells (effectors) from day-8 RSV-infected or mock-infected mice were incubated with EL4 target cells loaded with a peptide (RSV peptide or SeV control peptide). The target cells were differentially labeled with CFSE and incubated with the effector cells at the indicated effector : target (E:T) ratios for 4 hours. Cells were then analyzed by flow-cytometry and the specific killing of RSV peptide-loaded targets was calculated (n = 3 per group)

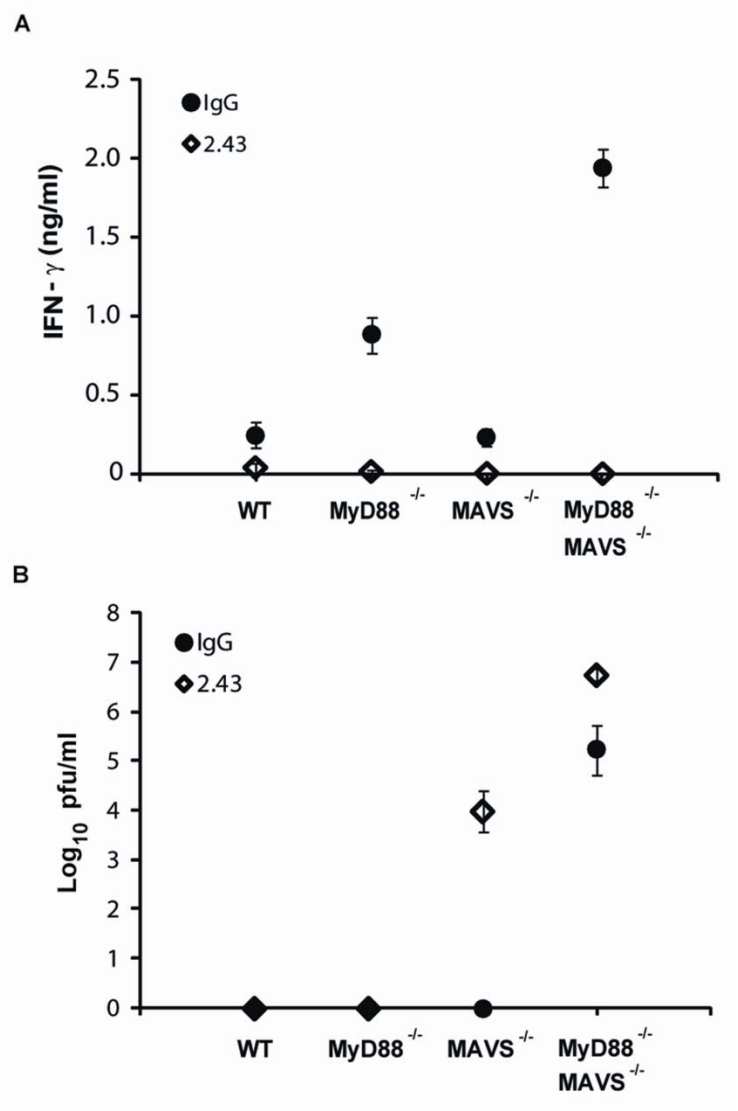

Figure 17. CD8$^+$ T cell depletion in RSV infected mice. (**A**) Mice were either depleted of CD8$^+$ T cells (with antibody 2.43) or mock depleted (IgG) and infected with RSV. BALF was extracted on day 8 and IFN-γ was measured by ELISA (n = 3 per group). (**B**) BALF viral titers were measured for mice described in (**A**). Data are represented as mean +/- SEM.

To investigate how *Mavs*$^{-/-}$ and DKO mice mount a largely normal CTL response in the absence of innate interferons and cytokines known to be important for activating adaptive immunity, we examined the activation of dendritic cells. We first measured up-regulation of CD86 in CD11c^{+} GM-CSF-derived BMDCs in response to RSV and SeV infection in vitro. CD86 up-regulation was observed in wild-type and *Myd88*$^{-/-}$ DCs but not in *Mavs*$^{-/-}$ and DKO DCs (Fig. 18), suggesting a complete dependence on MAVS-mediated signaling. As a control, LPS-induced CD86 surface expression was observed in DCs of all genotypes.

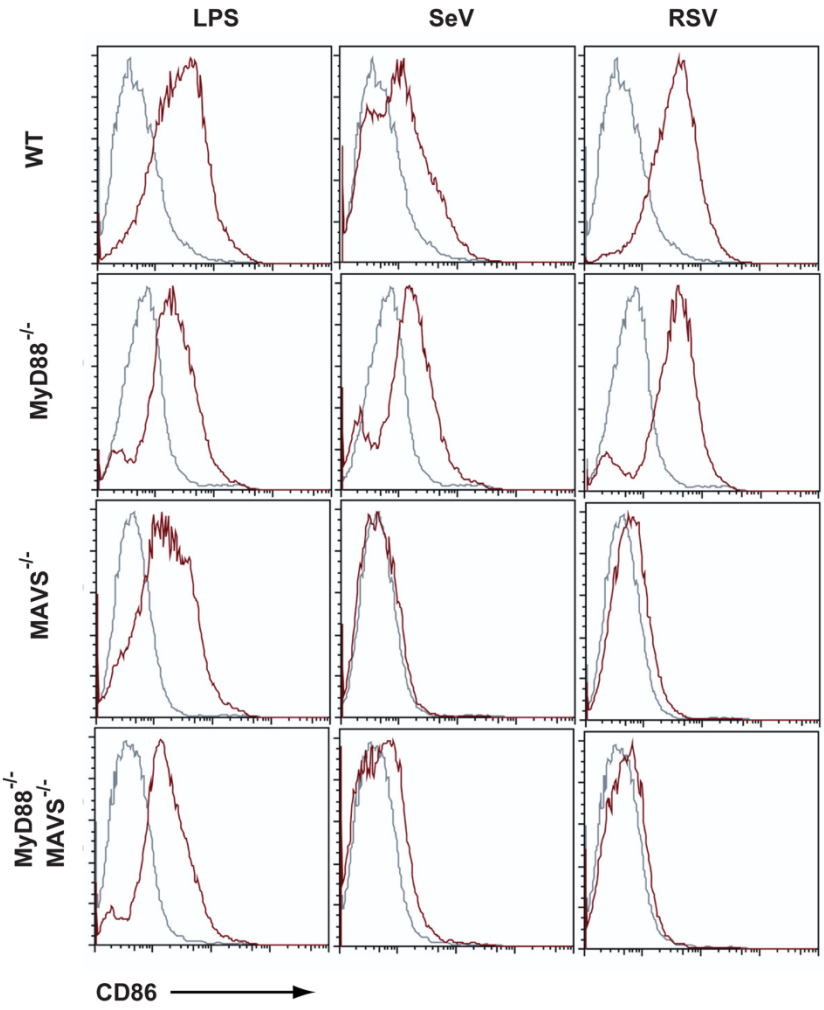

Figure 18. In vitro DC activation by RSV. Bone marrow-derived DC of the indicated genotypes were treated with LPS (1 μg/ml), RSV (MOI = 1) or SeV (50 HA U/ml) for 24 hours before surface CD86 expression was measured by flow cytometry. Gray histograms represent DCs treated with media and are overlaid with each of the other conditions shown in red.

Since the RSV-induced response in these cultured DCs did not explain intact $CD8^+$ T cell activation in mice lacking MAVS, we examined in vivo activation of pulmonary cDCs, which were identified as $CD11c^+$, $CD2^-$ and $F4/80^-$ cells (Kumagai, Takeuchi et al. 2007). Both wild-type and MyD88-deficient $CD11c^+$ DCs up-regulated surface levels of CD86 (Fig. 19A) and CD80 (data not shown) after RSV infection compared to mock infected mice. In both MAVS-deficient and DKO mice, up-regulation of these molecules was drastically reduced. However, a small percentage of the pulmonary DCs in these mice consistently up-regulated these molecules indicating their activation. In contrast, CD86 up-regulation was completely MAVS-dependent in $CD11c^+CD2^+F4/80^+$ alveolar macrophages of the same mice (Fig. 19A).

Following activation, antigen-loaded DCs traffic from their peripheral tissue location to draining lymph nodes where they activate T cells. Therefore, we examined the phenotype of DCs in the mediastinal lymph nodes draining the lung (Fig. 19B). Upon RSV infection, the majority of lymph node DCs in wild-type and *Myd88*$^{-/-}$ mice were $CD86^{high}$ compared to DCs in mock treated mice. Consistent with the notion that the subset of pulmonary DC activated in the absence of MAVS may subsequently traffic to the lymph node, we found a significant percentage of $CD86^{high}$ DCs in the lymph nodes of *Mavs*$^{-/-}$ and DKO mice. This subset of DCs may be responsible for the effective activation of RSV-

specific CTLs in the absence of innate immunity mediated by MAVS and MyD88.

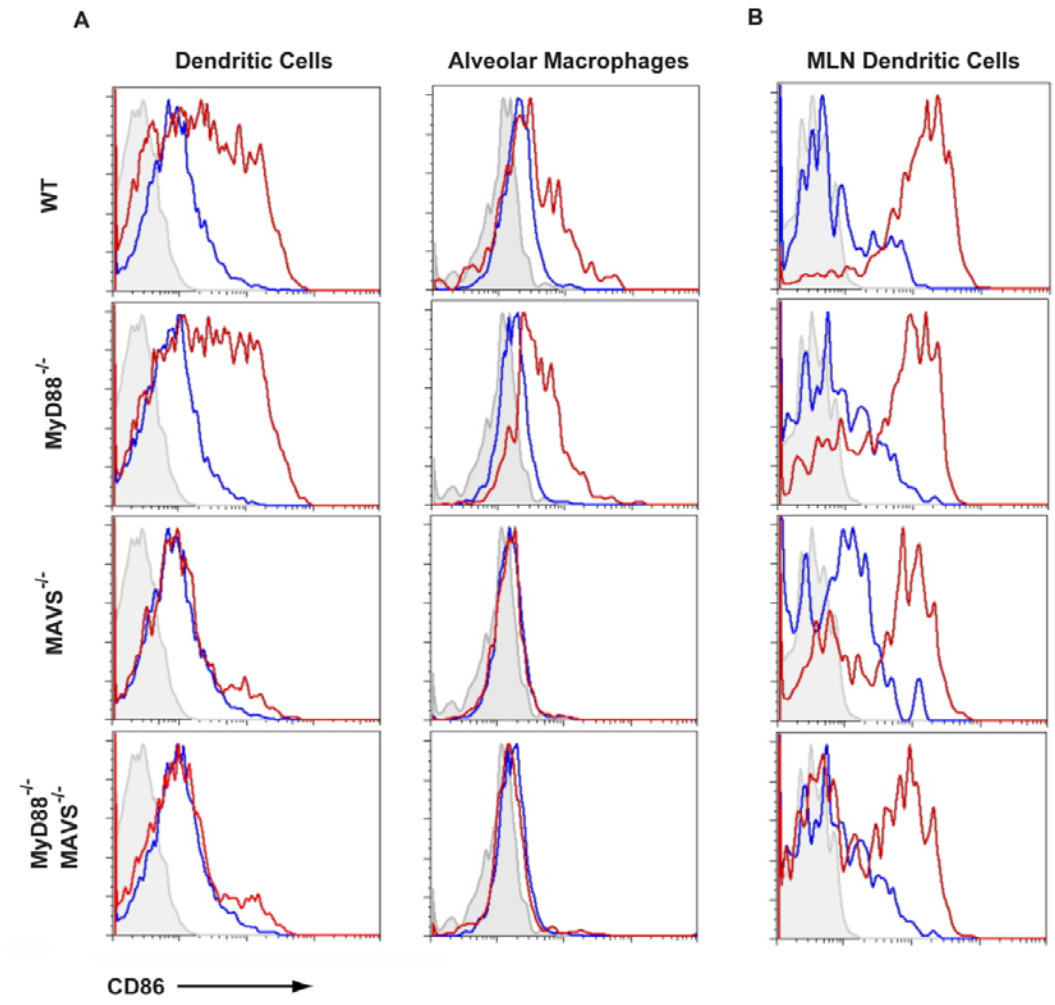

Figure 19. A subset of pulmonary DCs is activated by RSV in mice lacking *Mavs*. (A) Mice of the indicated genotypes were infected with RSV or mock treated for 24 hours before CD86 levels were assessed on pulmonary DCs and alveolar macrophages by flow cytometry. Shaded histograms represent isotype-control antibody staining, blue histograms represent DCs from mock infected mice and red histograms represent RSV infected mice. (**B**) Mediastinal lymph nodes (MLNs) were taken from mice described in (**A**) and surface expression of CD86 was assessed on dendritic cells by flow cytometry. Representative mice are shown for each genotype. (n=3 per group).

Conclusions

Despite such a drastically defective cytokine response and the fact that *Mavs*$^{-/-}$ mice harbored higher viral loads shortly after RSV infection, these mice still cleared the virus effectively by activating a normal CTL response. Antibody-mediated depletion of $CD8^+$ T cells significantly prolonged RSV replication, confirming their appropriate activation and demonstrating the important role of these cells in controlling the virus. While deletion of *Myd88* alone had no effect on RSV loads, mice lacking both adaptors had higher and more prolonged viral loads than those lacking either one alone, suggesting that in the absence of MAVS, MyD88 signaling contributed to antiviral immunity through a mechanism independent of IFN-I induction. Remarkably, even the DKO mice were able to activate $CD8^+$ T cells and clear the virus effectively.

It is surprising that $CD8^+$ T cell activation is normal in the absence of MAVS, as it is widely believed that IFN-I and cytokines produced during innate antiviral responses are required for activating adaptive immunity including cross-priming (Medzhitov and Janeway 1999; Hoebe, Janssen et al. 2004). A subset of pulmonary DCs is activated by RSV in the lung and then migrates to the mediastinal lymph nodes in the absence of MAVS and MyD88. It is possible that this subset of DCs is responsible for the cross-priming of $CD8^+$ T cells in a

manner that depends on TLR3 and TRIF. We have assessed the expression of several surface markers including CD8α, CD4, CD11b, B220, mPDCA1 and GR-1 on the pulmonary DC and found that none are specifically enriched or lower in the activated subset in the wild type mice or those lacking *Mavs* or *Myd88*. Therefore, it is still not clear what makes this subset of DCs unique in getting activated by RSV in the absence of MAVS and MyD88. Further characterization of this DC subset should provide important insights into the regulation of T cell responses to RSV and possibly other pathogens.

CHAPTER FOUR

SUMMARY

Since the discovery of mammalian TLRs about a decade ago, a significant amount of data has established the prominent role of these receptors in the initiation of innate responses to a broad range of pathogens including viruses. Beginning with the discovery of human TLRs, experimental evidence has also revealed an important role of this receptor family in the initiation and of adaptive immune responses (Medzhitov, Preston-Hurlburt et al. 1997). More recently, additional pathogen receptors and pathways have been uncovered including NLRs, RLRs and a DNA sensing pathway for which the receptor(s) remains unknown. How signals generated through these innate receptors affect innate and adaptive immune responses and how they integrate with TLR-derived signals is an important issue that is now beginning to be unraveled. At the initiation of the project presented here, the RLR pathway was implicated in the recognition of RNA viruses with MAVS as an essential component of this system. The initial studies of Mavs-deficient mice revealed compromised innate immunity to viruses such as SeV and VSV. One question that immediately followed was the relative importance of RLR signaling compared to TLRs in the host's innate and adaptive response to RNA-virus infection. We have shown that in response to the human pathogen, RSV, the RLR pathway plays a critical role in innate immune

induction, possibly more important than TLRs. The induction of IFN-I and most innate cytokines and chemokines is lost when the RLR pathway is disrupted. While disruption of RLR signaling abrogated induction of IFN-I and most innate chemokines and cytokines, an exhaustive study of innate immune activation has not been done and is warranted. Future studies will hopefully dissect the role of RLR signaling on the function of various innate immune cells including neutrophils and natural killer cells. Through the assessment of anti-RSV antibody responses we have also shown that, indeed, RLR signaling through MAVS may be required to activate certain aspects of adaptive immunity depending on the identity of the infecting pathogen. Our finding that primary CTL activation proceeds normally and that some pulmonary DCs are activated even in the absence of both MyD88 and MAVS is surprising and may reflect redundancy in our response to the virus. Further study of these activated DCs may reveal a novel subset of DCs which could be an important target for vaccines. Finally, we have clearly shown that an effective anti-RSV CTL response does not require MyD88 or MAVS. Finding out what these cells *do* need will add immensely to our understanding of basic CTL biology and may serve in the design of better RSV vaccines and adjuvants.

BIBLIOGRAPHY

Awomoyi, A. A., P. Rallabhandi, et al. (2007). "Association of TLR4 polymorphisms with symptomatic respiratory syncytial virus infection in high-risk infants and young children." J Immunol **179**(5): 3171-7.

Banchereau, J. and R. M. Steinman (1998). "Dendritic cells and the control of immunity." Nature **392**(6673): 245-52.

Boogaard, I., M. van Oosten, et al. (2007). "Respiratory syncytial virus differentially activates murine myeloid and plasmacytoid dendritic cells." Immunology **122**(1): 65-72.

Bowie, A. G. and K. A. Fitzgerald (2007). "RIG-I: tri-ing to discriminate between self and non-self RNA." Trends Immunol **28**(4): 147-50.

Chen, Z. J. (2005). "Ubiquitin signalling in the NF-kappaB pathway." Nat Cell Biol **7**(8): 758-65.

Chen, Z. J. (2005). "Ubiquitin signalling in the NF-κB pathway." Nature Cell Biology **7**(8): 758-766.

Collins, P. L. and B. R. Murphy (2005). "New generation live vaccines against human respiratory syncytial virus designed by reverse genetics." Proc Am Thorac Soc **2**(2): 166-73.

Connors, M., N. A. Giese, et al. (1994). "Enhanced pulmonary histopathology induced by respiratory syncytial virus (RSV) challenge of formalin-inactivated RSV-immunized BALB/c mice is abrogated by depletion of interleukin-4 (IL-4) and IL-10." J Virol **68**(8): 5321-5.

Connors, M., A. B. Kulkarni, et al. (1992). "Pulmonary histopathology induced by respiratory syncytial virus (RSV) challenge of formalin-inactivated RSV-immunized BALB/c mice is abrogated by depletion of CD4+ T cells." J Virol **66**(12): 7444-51.

Cowton, V. M., D. R. McGivern, et al. (2006). "Unravelling the complexities of respiratory syncytial virus RNA synthesis." J Gen Virol **87**(Pt 7): 1805-21.

Domachowske, J. B. and H. F. Rosenberg (1999). "Respiratory syncytial virus infection: immune response, immunopathogenesis, and treatment." Clin Microbiol Rev **12**(2): 298-309.

Ehl, S., R. Bischoff, et al. (2004). "The role of Toll-like receptor 4 versus interleukin-12 in immunity to respiratory syncytial virus." Eur J Immunol **34**(4): 1146-53.

Faisca, P., D. B. Tran Anh, et al. (2006). "Suppression of pattern-recognition receptor TLR4 sensing does not alter lung responses to pneumovirus infection." Microbes Infect **8**(3): 621-7.

Fitzgerald, K. A., S. M. McWhirter, et al. (2003). "IKKepsilon and TBK1 are essential components of the IRF3 signaling pathway." Nat Immunol **4**(5): 491-6.

Graham, B. S., L. A. Bunton, et al. (1991). "Respiratory syncytial virus infection in anti-mu-treated mice." J Virol **65**(9): 4936-42.

Graham, B. S., L. A. Bunton, et al. (1991). "Role of T lymphocyte subsets in the pathogenesis of primary infection and rechallenge with respiratory syncytial virus in mice." J Clin Invest **88**(3): 1026-33.

Hall, C. B. and C. A. McCarthy (2004). Mandell, Douglas, and Bennett's Principles and Practice of Infectious diseases. G. L. Mandell, J. E. Bennet and R. Dolin, Churchill Livingston. **2:** 2008-2021.

Hayden, M. S. and S. Ghosh (2008). "Shared principles in NF-kappaB signaling." Cell **132**(3): 344-62.

Haynes, L. M., D. D. Moore, et al. (2001). "Involvement of toll-like receptor 4 in innate immunity to respiratory syncytial virus." J Virol **75**(22): 10730-7.

Hoebe, K., E. Janssen, et al. (2004). "The interface between innate and adaptive immunity." Nat Immunol **5**(10): 971-4.

Hornung, V., J. Ellegast, et al. (2006). "5'-Triphosphate RNA is the ligand for RIG-I." Science **314**(5801): 994-7.

Horvath, A. K. a. C. M. (2006). "RNA- and Virus-Independent Inhibition of Antiviral Signaling by RNA Helicase LGP2." Journal of Virology **80**(24): 12332-12342.

Iwasaki, A. and R. Medzhitov (2004). "Toll-like receptor control of the adaptive immune responses." Nat Immunol **5**(10): 987-95.

Izaguirre, A., B. J. Barnes, et al. (2003). "Comparative analysis of IRF and IFN-alpha expression in human plasmacytoid and monocyte-derived dendritic cells." J Leukoc Biol **74**(6): 1125-38.

Jafri, H. S., S. Chavez-Bueno, et al. (2004). "Respiratory syncytial virus induces pneumonia, cytokine response, airway obstruction, and chronic inflammatory infiltrates associated with long-term airway hyperresponsiveness in mice." J Infect Dis **189**(10): 1856-65.

Jewell, N. A., N. Vaghefi, et al. (2007). "Differential type I interferon induction by respiratory syncytial virus and influenza a virus in vivo." J Virol **81**(18): 9790-800.

Jung, A., H. Kato, et al. (2007). "Lymphocytoid choriomeningitis virus activates plasmacytoid dendritic cells and induces cytotoxic T cell response via MyD88." J Virol.

Kanneganti, T. D., M. Lamkanfi, et al. (2007). "Intracellular NOD-like receptors in host defense and disease." Immunity **27**(4): 549-59.

Kato, H., S. Sato, et al. (2005). "Cell type-specific involvement of RIG-I in antiviral response." Immunity **23**(1): 19-28.

Kawai, T. and S. Akira (2006). "TLR signaling." Cell Death Differ **13**(5): 816-25.
Kim, H. W., J. G. Canchola, et al. (1969). "Respiratory syncytial virus disease in infants despite prior administration of antigenic inactivated vaccine." Am J Epidemiol **89**(4): 422-34.
Kumagai, Y., O. Takeuchi, et al. (2007). "Alveolar macrophages are the primary interferon-alpha producer in pulmonary infection with RNA viruses." Immunity **27**(2): 240-52.
Kurt-Jones, E. A., L. Popova, et al. (2000). "Pattern recognition receptors TLR4 and CD14 mediate response to respiratory syncytial virus." Nat Immunol **1**(5): 398-401.
Lee, M. S. and Y. J. Kim (2007). "Signaling pathways downstream of pattern-recognition receptors and their cross talk." Annu Rev Biochem **76**: 447-80.
Liu, Y. J. (2005). "IPC: professional type 1 interferon-producing cells and plasmacytoid dendritic cell precursors." Annu Rev Immunol **23**: 275-306.
Loo, Y. M., J. Fornek, et al. (2007). "Distinct Rig-I and Mda5 Signaling by Rna Viruses in Innate Immunity." J Virol.
Maniatis, T., J. V. Falvo, et al. (1998). "Structure and function of the interferon-beta enhanceosome." Cold Spring Harb Symp Quant Biol **63**: 609-20.
Medzhitov, R. and C. A. Janeway, Jr. (1999). "Innate immune induction of the adaptive immune response." Cold Spring Harb Symp Quant Biol **64**: 429-35.
Medzhitov, R., P. Preston-Hurlburt, et al. (1997). "A human homologue of the Drosophila Toll protein signals activation of adaptive immunity." Nature **388**(6640): 394-7.
Meylan, E., J. Curran, et al. (2005). "Cardif is an adaptor protein in the RIG-I antiviral pathway and is targeted by hepatitis C virus." Nature **437**(7062): 1167-72.
Murata, Y. and A. R. Falsey (2007). "Respiratory syncytial virus infection in adults." Antivir Ther **12**(4 Pt B): 659-70.
Openshaw, P. J., G. S. Dean, et al. (2003). "Links between respiratory syncytial virus bronchiolitis and childhood asthma: clinical and research approaches." Pediatr Infect Dis J **22**(2 Suppl): S58-64; discussion S64-5.
Parker, D. C. (1993). "T cell-dependent B cell activation." Annu Rev Immunol **11**: 331-60.
Pasare, C. and R. Medzhitov (2005). "Control of B-cell responses by Toll-like receptors." Nature **438**(7066): 364-8.
Pichlmair, A., O. Schulz, et al. (2006). "RIG-I-mediated antiviral responses to single-stranded RNA bearing 5'-phosphates." Science **314**(5801): 997-1001.

Prlic, M., M. A. Williams, et al. (2007). "Requirements for CD8 T-cell priming, memory generation and maintenance." Curr Opin Immunol **19**(3): 315-9.

Rothenfusser, S., N. Goutagny, et al. (2005). "The RNA helicase Lgp2 inhibits TLR-independent sensing of viral replication by retinoic acid-inducible gene-I." J Immunol **175**(8): 5260-8.

Rudd, B. D., E. Burstein, et al. (2005). "Differential role for TLR3 in respiratory syncytial virus-induced chemokine expression." J Virol **79**(6): 3350-7.

Rudd, B. D., M. A. Schaller, et al. (2007). "MyD88-mediated instructive signals in dendritic cells regulate pulmonary immune responses during respiratory virus infection." J Immunol **178**(9): 5820-7.

Rudd, B. D., J. J. Smit, et al. (2006). "Deletion of TLR3 alters the pulmonary immune environment and mucus production during respiratory syncytial virus infection." J Immunol **176**(3): 1937-42.

Rutigliano, J. A., M. T. Rock, et al. (2005). "Identification of an H-2D(b)-restricted CD8+ cytotoxic T lymphocyte epitope in the matrix protein of respiratory syncytial virus." Virology **337**(2): 335-43.

Saha, S. K., E. M. Pietras, et al. (2006). "Regulation of antiviral responses by a direct and specific interaction between TRAF3 and Cardif." Embo J **25**(14): 3257-63.

Saito, T., R. Hirai, et al. (2007). "Regulation of innate antiviral defenses through a shared repressor domain in RIG-I and LGP2." Proc Natl Acad Sci U S A **104**(2): 582-7.

Schlender, J., V. Hornung, et al. (2005). "Inhibition of toll-like receptor 7- and 9-mediated alpha/beta interferon production in human plasmacytoid dendritic cells by respiratory syncytial virus and measles virus." J Virol **79**(9): 5507-15.

Schwartz, R. H. (2003). "T cell anergy." Annu Rev Immunol **21**: 305-34.

Seth, R. B., L. Sun, et al. (2006). "Antiviral innate immunity pathways." Cell Res **16**(2): 141-7.

Seth, R. B., L. Sun, et al. (2005). "Identification and characterization of MAVS, a mitochondrial antiviral signaling protein that activates NF-kappaB and IRF 3." Cell **122**(5): 669-82.

Shohei Koyama, K. J. I., Himanshu Kumar, Takeshi Tanimoto, Cevayir Coban, Satoshi Uematsu, Taro Kawai, and Shizuo Akira (2007). "Differential Role of TLR- and RLR-Signaling in the Immune Responses to Influenza A Virus Infection and Vaccination." The Journal of Immunology **179**: 4711-4720.

Stark, G. R., I. M. Kerr, et al. (1998). "How cells respond to interferons." Annu Rev Biochem **67**: 227-64.

Sun, Q., L. Sun, et al. (2006). "The specific and essential role of MAVS in antiviral innate immune responses." Immunity **24**(5): 633-42.

Tamura, T., H. Yanai, et al. (2008). "The IRF family transcription factors in immunity and oncogenesis." Annu Rev Immunol **26**: 535-84.

Taro Kawai, K. T., Shintaro Sato, Cevayir Coban, Himanshu Kumar, Hiroki Kato, Ken J Ishii, Osamu Takeuchi, & Shizuo Akira (2005). "IPS-1, an adaptor triggering RIG-I- and Mda5-mediated type I interferon induction." Nature Immunology **6**: 981-988.

Thanos, D. and T. Maniatis (1995). "Virus induction of human IFN beta gene expression requires the assembly of an enhanceosome." Cell **83**(7): 1091-100.

Tulic, M. K., R. J. Hurrelbrink, et al. (2007). "TLR4 polymorphisms mediate impaired responses to respiratory syncytial virus and lipopolysaccharide." J Immunol **179**(1): 132-40.

Wang, H., N. Peters, et al. (2006). "Plasmacytoid dendritic cells limit viral replication, pulmonary inflammation, and airway hyperresponsiveness in respiratory syncytial virus infection." J Immunol **177**(9): 6263-70.

Waris, M. E., C. Tsou, et al. (1996). "Respiratory synctial virus infection in BALB/c mice previously immunized with formalin-inactivated virus induces enhanced pulmonary inflammatory response with a predominant Th2-like cytokine pattern." J Virol **70**(5): 2852-60.

Welliver, R. C. (2003). "Review of epidemiology and clinical risk factors for severe respiratory syncytial virus (RSV) infection." J Pediatr **143**(5 Suppl): S112-7.

Williams, M. A. and M. J. Bevan (2007). "Effector and memory CTL differentiation." Annu Rev Immunol **25**: 171-92.

Xu, L. G., Y. Y. Wang, et al. (2005). "VISA is an adapter protein required for virus-triggered IFN-beta signaling." Mol Cell **19**(6): 727-40.

Yamamoto, M., S. Sato, et al. (2003). "Role of adaptor TRIF in the MyD88-independent toll-like receptor signaling pathway." Science **301**(5633): 640-3.